

AD-A056 955

ALABAMA UNIV IN HUNTSVILLE

F/G 20/6

FINAL REPORT. 15 JUNE 1975 THROUGH 31 DECEMBER 1976, PART I, (U)

FEB 77 J A HARRINGTON, D A GREGORY, W OTTO

N00014-75-C-1158

UNCLASSIFIED

UAH-RR-198-PT-1

NL

| OF |  
AD  
A056955



END  
DATE  
FILMED

9 -78

DDC

AD A 056955

AD No. \_\_\_\_\_  
DDC FILE COPY

The University of Alabama in Huntsville

P. O. Box 1247  
Huntsville, Alabama 35807

Final Report

N00014-75-C-1158

By

James A. Harrington  
Principal Investigator

Prepared for

Naval Research Laboratory  
4555 Overlook Ave., S. W.  
Washington, D. C. 20375

February 1977

DISTRIBUTION STATEMENT A

Approved for public release;  
Distribution Unlimited

12

LEVEL II

DDC  
RECEIVED  
DEC 13 1977  
B

SECURITY CLASSIFICATION OF THIS PAGE (When Data Entered)

REPORT DOCUMENTATION PAGE		READ INSTRUCTIONS BEFORE COMPLETING FORM
1. REPORT NUMBER	2. GOVT ACCESSION NO.	3. RECIPIENT'S CATALOG NUMBER
4. TITLE (and Subtitle) None (Five reprints)		5. TYPE OF REPORT & PERIOD COVERED Final Report 15 June 75 - 31 Dec 76
7. AUTHOR(s) James A. Harrington et al		6. PERFORMING ORG. REPORT NUMBER UAH Research Report No. 198
9. PERFORMING ORGANIZATION NAME AND ADDRESS The University of Alabama in Huntsville P. O. Box 1247, Huntsville, AL 35807		8. CONTRACT OR GRANT NUMBER(s) N00014-75-C-1158
11. CONTROLLING OFFICE NAME AND ADDRESS Naval Research Laboratory 4555 Overlook Avenue, S.W., Washington, DC 20375		10. PROGRAM ELEMENT, PROJECT, TASK AREA & WORK UNIT NUMBERS
14. MONITORING AGENCY NAME & ADDRESS (if different from Controlling Office)		12. REPORT DATE February 1977
		13. NUMBER OF PAGES 35
		15. SECURITY CLASS. (of this report) UNCLASSIFIED
		15a. DECLASSIFICATION/DOWNGRADING SCHEDULE
16. DISTRIBUTION STATEMENT (of this Report) Approved for public release - distribution unlimited		
17. DISTRIBUTION STATEMENT (of the abstract entered in Block 20, if different from Report)		
18. SUPPLEMENTARY NOTES		
19. KEY WORDS (Continue on reverse side if necessary and identify by block number) Windows, infrared, absorption		
20. ABSTRACT (Continue on reverse side if necessary and identify by block number) The main objective of this research program is to study the optical properties of materials suitable for use as low loss windows and other optical components in the HF, DF and CO <sub>2</sub> laser wavelength regions. <span style="float: right;">(over)</span>		



In order to investigate these materials, measurements of the absorption coefficient were undertaken using laser calorimetry and infrared spectroscopy. To further this investigation, absorption at the surfaces of window materials was measured. This involved solving the classical heat flow problem using parameters gained from the experiment.

The study of extrinsic absorption was carried out using data at three wavelengths. From the observed absorption coefficients it seems a rather broad absorption band is centered in the HF and DF laser wavelength region. This band is not yet definitely understood nor identified.

Lastly, a study of the absorption of  $\text{ThO}_2$  - doped  $\text{Y}_2\text{O}_3$  was performed. This involved varying the preparation and final treatment of the samples to maximize transmission at the HF and DF laser wavelengths.

EXEMPTION		
WFO	Whole Section	<input checked="" type="checkbox"/>
BOC	Page Section	<input type="checkbox"/>
UNANNOUNCED		
JUSTIFICATION		
DISTRIBUTION/AVAILABILITY CODES		
Dist.	Avail.	and/or SPECIAL
A		



(14) UAH-RR-  
UAH Research Report No. 198 PT-1

The University of Alabama in Huntsville

P. O. Box 1247  
Huntsville, Alabama 35807

(6) Final Report

15 June 1975  
through  
31 December  
1976,  
Part I,

(15) N00014-75-C-1158

(10) By

James A. Harrington,  
Principal Investigator

Don A. Gregory,  
William /OHa,  
Charles E. /Patty, Jr.  
Donald R. /Hulsey

Prepared for

Naval Research Laboratory  
4555 Overlook Ave., S. W.  
Washington, D. C. 20375

(11) Feb 1977

(12) x3p.

389 469

15

## PREFACE

This report describes work on Low Loss Window Materials for Chemical Lasers under contract N00014-75-C-1158. This is a final report prepared for the Naval Research Laboratory, Washington, D. C. Participating in the research were, in addition to the principal investigator, James A. Harrington, Don A. Gregory, William Otto, Charles E. Patty, Jr., and Donald R. Hulsey.

### SUMMARY

The main objective of this research program is to study the optical properties of materials suitable for use as low loss windows and other optical components in the HF, DF and CO<sub>2</sub> laser wavelength regions.

In order to investigate these materials, measurements of the absorption coefficient were undertaken using laser calorimetry and infrared spectroscopy. To further this investigation, absorption at the surfaces of window materials was measured. This involved solving the classical heat flow problem using parameters gained from the experiment.

The study of extrinsic absorption was carried out using data at three wavelengths. From the observed absorption coefficients it seems a rather broad absorption band is centered in the HF and DF laser wavelength region. This band is not yet definitely understood nor identified.

Lastly, a study of the absorption of ThO<sub>2</sub> - doped Y<sub>2</sub>O<sub>3</sub> was performed. This involved varying the preparation and final treatment of the samples to maximize transmission at the HF and DF laser wavelengths.



## TABLE OF CONTENTS

Preface

Summary

Reprints

Infrared Absorption in Chemical Laser Window Materials

Infrared Bulk and Surface Absorption by Nearly Transparent  
Crystals

Infrared Absorption Limits of HF and DF Laser Windows

Extrinsic Absorption in KCl and KBr at CO<sub>2</sub> Laser Frequencies

Infrared Absorption in ThO<sub>2</sub>-Doped Y<sub>2</sub>O<sub>3</sub>

Conclusions

# Infrared absorption in chemical laser window materials

James A. Harrington, Don A. Gregory, and William F. Otto, Jr.

The optical absorption has been measured at DF and HF wavelengths in a wide variety of transparent materials that show promise for use as windows on high powered chemical lasers. These measurements, which were made using DF-HF chemical laser calorimetric methods, will be discussed in terms of surface and bulk contributions to the total absorption as well as in terms of the total absorption measured for each type of material studied. Materials studied include the alkaline earth fluorides, alkali halides, Ge, Si, ZnSe, MgO, Yttralox, and  $\text{Al}_2\text{O}_3$ .

## I. Introduction

The increasing interest and importance of chemical lasers have led to a demand for studies of optical materials at the DF and HF chemical laser frequencies. In particular, high energy chemical lasers will require low-loss optical materials for applications as windows and other transparent optical components. In order to help meet this demand, an investigation of the optical absorption coefficient for a wide variety of candidate chemical laser window materials was undertaken. In conjunction with the absorption measurements, chemical cleaning and polishing techniques have been developed and applied to some materials to determine their effectiveness in minimizing surface absorption.

Over the past several years, a continuing survey has been made of the most promising materials for operation at DF (3.8- $\mu\text{m}$ ) and HF (2.7- $\mu\text{m}$ ) wavelengths. In addition to categorizing the optical absorption  $\beta$  of many samples, it has become necessary to more carefully analyze  $\beta$  in terms of surface and bulk contributions to the total absorption. This is due to the fact that most of the desirable materials for use as DF laser windows have  $\beta$ 's that are extrinsically limited, and thus a prime emphasis of this work has been on the characterization and elimination of extrinsic (surface, impurity, etc.) absorption mechanisms.

Having surveyed a large number of materials it is now possible to bring together in a systematic way all results of our measurements of the absorption coefficient at chemical laser frequencies. One important point can be observed from such a compilation of data: no sample measured to date has a total  $\beta$  less than  $10^{-4} \text{ cm}^{-1}$  at either HF or DF frequencies. This is rather perplexing

in view of the fact that most materials of interest have intrinsic (multiphonon) levels far below this value and that, for some hosts,  $\beta$ 's less than  $10^{-4} \text{ cm}^{-1}$  have been measured at 5.25  $\mu\text{m}$  (Ref. 1) and 1.06  $\mu\text{m}$ .<sup>2</sup> It is felt that a major reason for this lies in the higher surface absorptions encountered at chemical laser frequencies. In addition to the obvious problem of  $\text{OH}^-$  contamination at HF wavelengths, it has been found that most organics commonly used to clean surfaces of window samples have strong absorption bands in the DF to HF region. In some cases it has been observed that chemical cleaning with an appropriate solvent just prior to measurement can reduce the absorption by one half of its value prior to cleaning. This sensitivity to chemical cleaning is not shared by materials measured at 5.25  $\mu\text{m}$  or 1.06  $\mu\text{m}$ , and it is probably for this reason that absorption coefficients are lower there than at chemical laser frequencies. Efforts will be reported on the methods used to minimize this source of absorption.

A review of the experimental techniques used to measure the small residual absorption in highly transparent materials will be given in the next section. This section will also include the procedures employed in handling and preparing the samples for measurement. Following this, experimental results will be given in Sec. III for all materials studied. Finally, a summary of results will be given along with recommendations of the best materials at the present time for use as low-loss chemical laser windows.

## II. Experimental Techniques and Procedures

### A. Laser Calorimetry

Standard laser calorimetric methods<sup>3</sup> were employed to measure the small absorption coefficients at chemical laser frequencies. The experimental arrangement consisted of either an air or vacuum calorimeter and a small cw DF-HF chemical laser of our own construction. This laser, which is similar in design to one built by

The authors are with University of Alabama, Physics Department, Huntsville, Alabama 35807.  
Received 2 February 1976.



Hinchen,<sup>4</sup> is of the SF<sub>6</sub> variety, delivering from 5 W to 10 W of cw multiline HF power and about 6 W of cw multiline DF power. The calorimeters are conventional<sup>1</sup> except for a series of small holes along the bottom that admit dry nitrogen purge gas to the air calorimeter when it is used for HF measurements. In practice, the absorption of HF radiation by air in the calorimeter and subsequent distortion of the heating-cooling curves due to heating of the air have not been detected even without the purge. Purge gas is frequently used, however, to minimize any errors in the temperature-time data and in measuring the laser power. The vacuum calorimeters are used for the hydroscopic materials.

A three-slope method<sup>3</sup> is applied to the data for the calculation of  $\beta$ . The fractional power absorbed at the surfaces has been measured by two different techniques. The first is an older method in which the total absorption is measured as a function of sample length  $L$ . An extrapolation of a plot of  $\beta L$  vs  $L$  to zero length then gives a measure of the loss per surface while the slope gives the bulk  $\beta$ . The other method<sup>5</sup> was developed by Hass and involves measuring the absorption in long, bar-shaped samples. With the appropriate sample geometry it is possible to distinguish between surface and bulk absorption directly from slope changes in the temperature-time curves.

#### B. Sample Procurement and Preparation

The samples studied have been procured from a wide variety of window material processors. In most cases the samples are received with a good surface finish. When this is the case, the sample is run as-received in order to obtain a  $\beta$  unbiased by any of our polishing and cleaning techniques. After an initial measurement, the surfaces are examined using Nomarski microscopy and then refinished. Mechanical polishing involves a final polish with Linde B and isopropanol with intermediate polishes using diamond grit for the harder substances. For ZnSe, a potassium ferricyanide chemical etch and polishing on pitch laps was used.

Surface cleaning just prior to measurement is one of the most important requirements for a reliable  $\beta$ . Popular CH-bonded solvents like methanol, ethanol, acetone, etc., which have absorptions in the DF-HF region, have been found to produce higher absorption coefficients in crystals washed with these than for crystals washed in, for example, carbon tetrachloride. At the present time, all crystals have a final cleaning in spectrograde CCl<sub>4</sub>. With a good surface finish and careful cleaning it has, on occasion, been possible to reduce the total  $\beta$  of the as-received sample by more than one-half of its original value. Cases where this occurs are indicated in the explicit results that follow.

### III. Experimental Results and Discussion

#### A. Zinc Selenide

An important material at 10.6  $\mu$ m, zinc selenide holds great promise as a window at chemical laser frequencies as well. This material has a negligible intrinsic absorption at 3.8  $\mu$ m, and thus it is expected that the

DF-HF absorption coefficients will be extrinsically limited. All ZnSe studied is polycrystalline, CVD grown material obtained from Raytheon Research Labs.

The oldest sample, grown several years ago, was ZnSe-96. This sample had a total  $\beta$  equal to  $3 \times 10^{-3}$  cm<sup>-1</sup> at 10.6  $\mu$ m but had absorption coefficients almost ten times greater at DF and HF wavelengths:

$$\beta(\text{DF}) = 3.3 \times 10^{-2} \pm 4\% \text{ cm}^{-1},$$

$$\beta(\text{HF}) = 2.2 \times 10^{-2} \pm 7\% \text{ cm}^{-1}.$$

These values were obtained from the as-received sample, and no further work was pursued on this piece because better material was being received. In particular, ZnSe-96 exhibited the usual light-dark bands which often characterized Raytheon's early material. It was decided to concentrate on the more recent ZnSe which was free of these obvious bands.

The next sample received for study was part of Raytheon's absorption standard series (No. 40). This sample had a total  $\beta$  equal to  $1.98 \times 10^{-3} \pm 4\% \text{ cm}^{-1}$  at 10.6  $\mu$ m as measured by us ( $1.69 \times 10^{-3} \text{ cm}^{-1}$  as measured by Raytheon at 10.6  $\mu$ m). Our value is that measured after cleaning the surfaces in methanol. On the as-received sample the 10.6- $\mu$ m absorption was measured to be  $2.48 \times 10^{-3} \text{ cm}^{-1}$ . Here is an example of the effect of a simple chemical cleaning on the total  $\beta$ . In this case the absorption was reduced by about 50% by the methanol wash. The absorption at chemical laser wavelengths was found to be substantially reduced from the high values previously measured in ZnSe-96. The total  $\beta$ 's were found to be

$$\beta(\text{DF}) = 2.2 \times 10^{-3} \text{ cm}^{-1},$$

$$\beta(\text{HF}) = 4.0 \times 10^{-3} \text{ cm}^{-1},$$

for the sample after the methanol wash.

Even though the absorption was reduced to the low  $10^{-3}$ -cm<sup>-1</sup> region at DF-HF frequencies, this was still far above the intrinsic level for this material. In order to determine how much of this absorption was due to the surfaces a third sample was obtained from Raytheon (Run I-20). This rectangular parallelepiped was cut into four lengths for  $\beta L$  vs  $L$  measurements at 10.6  $\mu$ m, 3.8  $\mu$ m, and 2.7  $\mu$ m.

For the DF-HF wavelength measurements the sample surfaces were mechanically polished using diamond grits with a final polish using Linde B and isopropanol. All surfaces were cleaned prior to measuring with spectrograde CCl<sub>4</sub>. For the CO<sub>2</sub> calorimetry, the above finishes were further refined using a chemical etch (potassium ferricyanide). An important consideration in all these measurements was that the surfaces were all treated identically for each series of measurements at a given laser frequency.

The  $\beta L$  vs  $L$  plots for all three laser wavelengths are shown in Fig. 1. A least squares fit was made to the data, and the following  $\beta$ 's extracted are listed in Table I along with the earlier ZnSe results which are summarized for completeness. The surface absorption shown represents the fractional power loss for two surfaces.

Several important features can be gleaned from the



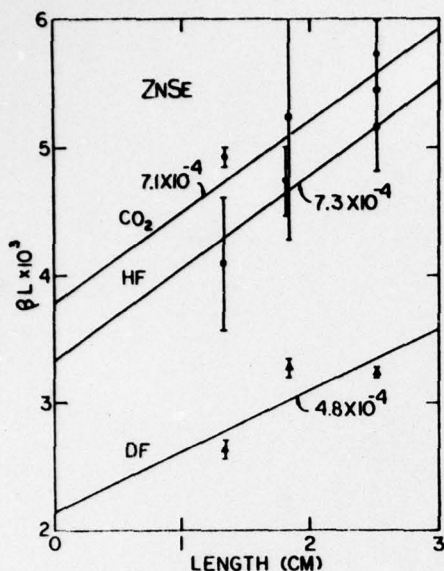


Fig. 1. Determination of surface and bulk absorption in Raytheon CVD ZnSe at CO<sub>2</sub>, DF, and HF laser frequencies.

results in Table I. The first is that for the two most recent ZnSe samples supplied by Raytheon, No. 40 and I-20, the total absorption is about the same for all three laser lines. It is a little higher at HF, but this may be due to the presence of OH<sup>-</sup> in the bulk or on the surface of the samples. In a further reduction of the data into surface and bulk contributions, we see the surprisingly large surface absorption which dominates the total  $\beta$ . It is clear that a marked decrease in  $\beta_{\text{surf}}$  would mean a much improved window material since the  $\beta_{\text{bulk}}$  is quite good.

#### B. Silicon and Germanium

To investigate further the optical properties of semiconductors, several samples of silicon and one germanium sample were studied. The single crystal silicon came from Wacker Chemical Company in Germany and was P type with a high resistivity of 15,000  $\Omega$ -cm. A sample of low resistivity (14.5  $\Omega$ -cm), polycrystal silicon was obtained for comparison from Unique Optical.

The results of the chemical laser calorimetric measurements are shown in Table II. Commercial chemical

Table I. Absorption Coefficients for ZnSe at CO<sub>2</sub>, DF, and HF Wavelengths

Sample	Wavelength ( $\mu\text{m}$ )	$\beta_{\text{total}} (\text{cm}^{-1})$	$\beta_{\text{bulk}} (\text{cm}^{-1})$	$\beta_{\text{surface}}$
ZnSe-96	10.6	$3.0 \times 10^{-3}$	—	—
	3.8	$2.2 \times 10^{-2}$	—	—
	2.7	$3.3 \times 10^{-2}$	—	—
Std. No. 40	10.6	$1.98 \times 10^{-3} \pm 4\%$	—	—
	3.8	$2.2 \times 10^{-3}$	—	—
	2.7	$4.0 \times 10^{-3}$	—	—
I-20	10.6	$2.62 \times 10^{-3}$	$7.12 \times 10^{-4} \pm 10\%$	$3.8 \times 10^{-3} \pm 10\%$
	3.8	$2.62 \times 10^{-3}$	$4.8 \times 10^{-4}$	$2.14 \times 10^{-3}$
	2.7	$4.05 \times 10^{-3}$	$7.34 \times 10^{-4}$	$3.32 \times 10^{-3}$

Table II. Absorption Coefficients for Ge and Si at DF and HF Wavelengths

Sample	Wavelength ( $\mu\text{m}$ )	$\beta_{\text{total}} (\text{cm}^{-1})$	Comments
Ge (Cal Tech)	3.8	$1.6 \times 10^{-2}$	Before polish
		$1.35 \times 10^{-2} \pm 4\%$	After polish
	2.7	$1.6 \times 10^{-2}$	Before polish
Si (Cal Tech)		$1.3 \times 10^{-2} \pm 1\%$	After polish
	3.8	$7.85 \times 10^{-4} \pm 6\%$	15,000 $\Omega$ -cm
	2.7	$5.5 \times 10^{-3} \pm 2\%$	
Si (Unique Optical)	3.8	$2.53 \times 10^{-1} \pm 3\%$	14.5 $\Omega$ -cm
	2.7	$1.4 \times 10^{-1} \pm 3\%$	

Table III. Strontium Fluoride (Raytheon-Cast)

Sample No.	Length (cm)	Total absorption coefficient ( $\text{cm}^{-1}$ )		Comment
		DF	HF	
VHP-275	—	$8 \times 10^{-4}$	$1.4 \times 10^{-3}$	Inhomogeneous
VHP-348	4.44	$7.0 \times 10^{-4}$	$6.3 \times 10^{-4}$	As received
	1.88	$10 \times 10^{-4}$	$16 \times 10^{-4}$	
	0.86	$12 \times 10^{-4}$	$19 \times 10^{-4}$	
	4.44	$4.1 \times 10^{-4}$	$3.8 \times 10^{-4}$	Repolished
	1.88	$7.7 \times 10^{-4}$	$11 \times 10^{-4}$	
VHP-400	0.86	$17 \times 10^{-4}$	$24 \times 10^{-4}$	
	1.0	$3.5 \times 10^{-4}$	$3.3 \times 10^{-3}$	Test window sample

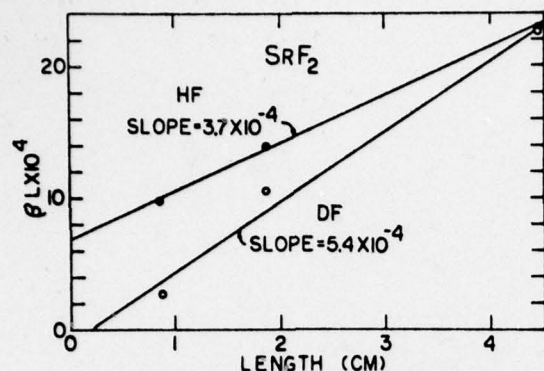


Fig. 2. Determination of surface and bulk absorption in Raytheon cast  $\text{SrF}_2$  at DF and HF laser frequencies.

polishes were applied to both the germanium and silicon samples. Before and after polish measurements are shown for germanium, only the after polish for silicon. No polish was applied to the silicon from Unique Optical due to the high absorption.

### C. Strontium Fluoride

Strontium fluoride has the potential of being one of the best window materials at chemical laser wavelengths owing to partially compensating physical parameters. In terms of figure of merit this means a large power may be transmitted before the window fractures or optically distorts the beam.<sup>6</sup> Most of the effort on  $\text{SrF}_2$  has been restricted to the cast polycrystalline  $\text{SrF}_2$  provided by Raytheon Research Labs.

The first sample studied was an irregular shaped piece, VHP-275. Unfortunately, inhomogeneities in  $\beta$  were detected across the sample, but representative values are given in Table III. This sample was not pursued further due to the inhomogeneities found in  $\beta$ .

The major portion of the effort on this host was devoted to Raytheon  $\text{SrF}_2$  (VHP-348). This rectangular parallelepiped ( $0.86 \times 1.88 \times 4.44$  cm) was used to obtain  $\beta L$  vs  $L$  data. The first set of data taken were on the as-received sample. Then due to some unusual discrepancies observed in  $\beta$  for the various lengths (discussed below) and because the surfaces as viewed by Nomarski microscopy were rather scratched, the surfaces were repolished. The repolishing involved using Linde B and distilled water followed by a  $\text{CCl}_4$  rinse.

The results for the as-received and repolished  $\text{SrF}_2$

sample are given in Table III for each length. From these results it is easily seen that there is consistent nonuniformity in the  $\beta$  values between the longest side (4.44 cm) and the other two sides at either DF or HF frequencies. This makes a plot of  $\beta L$  vs  $L$  meaningless, and thus no such plots are shown of these data.

In order to investigate this anisotropy in the absorption coefficient and, in particular, to determine if it is due to some surface effect, a vacuum cleaning of the sample was tried. The sample was soaked at  $300^\circ\text{C}$  in a  $10^{-6}$ -Torr vacuum for several hours before being placed in a vacuum calorimeter for measurement. On remeasuring the absorption, the total absorption for each length was in better agreement. These data are plotted on a  $\beta L$  vs  $L$  plot in Fig. 2. A least squares fit through the data yields slopes with bulk  $\beta$ 's in the mid  $10^{-4}\text{-cm}^{-1}$  range for both DF and HF frequencies. The data still show too much scatter, however, to be useful in determining a reliable surface absorption.

Table III also shows results on one of several 5-cm (2-in.) diam by 1-cm thick disks (VHP-400) of the most recent material supplied by Raytheon. This material has a very low total  $\beta$ .

### D. Alkaline Earth Fluorides—General

Several  $\text{CaF}_2$  samples were acquired from Hughes Research Laboratories for measurement. The samples received were forged  $\text{CaF}_2$  and single crystal  $\text{CaF}_2$ . All were polished and chemically cleaned then potted with a plastic film prior to shipping. Just prior to measurement, this protective coating was removed. It was observed in some cases that on further cleaning the absorption went down. This may be due to the removal of a residue left on the surface by the plastic film.

The results for several samples are listed in Table IV along with comments pertaining to the type of surface finish used. From the table it can be seen that the single crystal material has a slightly lower absorption than the forged material. In fact the single crystal material is the lowest DF  $\beta$  measured to date in  $\text{CaF}_2$ . Another piece of forged  $\text{CaF}_2$  in the shape of a long bar has indicated, however, that the  $\beta$  in the forged material is not always so high.

The results for the total absorption in a variety of commercial alkaline earth fluoride samples are compiled in Table V. These results clearly indicate the variation still present in  $\beta$ 's obtained from different vendors. It is expected that these fluctuations will become smaller in time as materials processing of these hosts improves.

Table IV. Calcium Fluoride  
(Hughes Research Laboratory)

Sample	Comment	Absorption coefficient	
		DF	HF
H1309-74	Forged bar	$2.7 \times 10^{-4}$ (bulk) $\text{cm}^{-1}$	$1.8 \times 10^{-4}$ (bulk) $\text{cm}^{-1}$
		$1.3 \times 10^{-4}$ (two surfaces)	$2.8 \times 10^{-4}$ (two surfaces)
H1309-24	Forged disk	$1.3 \times 10^{-3}$ $\text{cm}^{-1}$	$3.0 \times 10^{-3}$ $\text{cm}^{-1}$
H1309-07-A	Single crystal		
	As received	$5.5 \times 10^{-4}$ $\text{cm}^{-1}$	$9.3 \times 10^{-4}$ $\text{cm}^{-1}$
	Repolished	$1.7 \times 10^{-4}$ $\text{cm}^{-1}$	$4.9 \times 10^{-4}$ $\text{cm}^{-1}$



Table V. Alkaline Earth Fluorides

Host	Supplier	Absorption coefficient ( $\text{cm}^{-1}$ )	
		DF	HF
$\text{CaF}_2$	Adolf Meller	$21 \times 10^{-4}$	$2.2 \times 10^{-3}$
$\text{CaF}_2$	Raytheon	$6.0 \times 10^{-4}$	$1.5 \times 10^{-3}$
$\text{CaF}_2$	Harshaw	$2.7 \times 10^{-4}$	$5.2 \times 10^{-3}$
$\text{CaF}_2$	Optovac	$5.9 \times 10^{-4}$	$0.78 \times 10^{-3}$
$\text{BaF}_2$	Adolf Meller	$2.0 \times 10^{-4}$	$0.11 \times 10^{-3}$
$\text{BaF}_2$	Optovac	$20 \times 10^{-4}$	$1.8 \times 10^{-3}$
$\text{SrF}_2$	Optovac	$9.5 \times 10^{-4}$	$1.5 \times 10^{-3}$
$\text{MgF}_2$	Optovac	$4.6 \times 10^{-4}$	$0.86 \times 10^{-3}$

Table VI. Absorption Coefficients for NaF at DF and HF Wavelengths

Sample	Wavelength ( $\mu\text{m}$ )	$\beta_{\text{total}}$ ( $\text{cm}^{-1}$ )
NaF:Li (NRL 960)	3.8	$7 \times 10^{-4}$
	2.7	$9 \times 10^{-4}$
NaF (2nd Gen. No. 11)	3.8	$2.7 \times 10^{-4}$
	2.7	$4.3 \times 10^{-4}$

Table VII. Multiline Chemical Laser Output

DF ( $\mu\text{m}$ )	HF ( $\mu\text{m}$ )
3.75	2.738
3.837	2.906
3.876	2.866
	2.777
	2.818

## E. Sodium Fluoride

Two samples of NaF received from the Naval Research Laboratory were studied in detail. One sample had a small amount of Li (1 mole %) added to the melt. The other was a pure, second generation grown ingot. The results for both samples are given in Table VI. In each case the values given represent the average value after repolishing the samples and chemical cleaning just prior to measurement.

Quite clearly, the purer, second generation NaF has lower over-all absorption as might be expected *a priori*.

One reason for this is the reduction of the  $\text{OH}^-$  concentration which occurs in the second generation growth process. A reduction of the  $\text{OH}^-$  has correspondingly reduced the HF absorption. One can be even more specific and look at the position of the main  $\text{OH}^-$  band in NaF which occurs at  $2.78 \mu\text{m}$  (Ref. 7) and compare this with the multiline HF laser output. Table VII contains a partial list of the frequencies present in our multiline output (strongest to weakest). One sees that indeed the strongest HF lines are very near the  $\text{OH}^-$  line in NaF. The lines at  $2.738 \mu\text{m}$  and  $2.777 \mu\text{m}$  should be strongly absorbed by the  $\text{OH}^-$ , and thus a measurement of the HF  $\beta$  is an indication of the  $\text{OH}^-$  impurity content in the crystal.

## F. Miscellaneous Alkali Halides

In this section we shall summarize the results of absorption coefficient measurements on LiF, NaCl, KCl, KBr, and KRS-5. Both polycrystalline (P) and single crystal (S) samples received from several vendors were studied. All materials (except KRS-5) were polished just prior to measurement, and chemical etches were applied to KCl and KBr.<sup>8</sup> The chemical etch not only helps reduce surface absorption but also passivates, to some extent, the surfaces against atmospheric moisture.

The results for these hosts are given in Table VIII. The data for LiF indicate the intrinsic nature of this salt at DF frequencies. Deutsch<sup>9</sup> has published a  $\beta$  vs  $\omega$  curve for LiF, and from this we extract an intrinsic  $\beta = 1 \times 10^{-3} \text{ cm}^{-1}$  at around  $3.8 \mu\text{m}$ . The frequency spread of the DF multiline output influences the  $\beta$  value measured since our value is an average over this small frequency range. Thus the average DF  $\beta$  in LiF of about  $1.8 \times 10^{-3} \text{ cm}^{-1}$  is essentially intrinsic with the difference between  $\beta_{\text{meas}}$  ( $1.8 \times 10^{-3} \text{ cm}^{-1}$ ) and  $\beta_{\text{int}}$  ( $1 \times 10^{-3} \text{ cm}^{-1}$ ) being mostly due to the frequency spread of the multiline laser output used in the measurements.

The Polytran NaCl has a very low DF absorption—one of the lowest measured  $\beta$ 's of any crystal studied to date. KCl and KBr also exhibit a low bulk  $\beta$ . In general, the alkali halides show some of the smallest  $\beta$ 's measured at DF-HF wavelengths.

## G. Yttralox

Yttralox is a cubic, polycrystalline ceramic (90%  $\text{Y}_2\text{O}_3$  and 1  $\text{ThO}_2$ )<sup>10</sup> which shows increasing potential as a

Table VIII. Miscellaneous Alkali Halides

Host	Supplier	Absorption coefficient	
		DF	HF
NaCl (P)	Harshaw	$1.5 \times 10^{-4} \text{ cm}^{-1}$	$1.8 \times 10^{-3} \text{ cm}^{-1}$
NaCl (S)	Harshaw-Bar	$5.9 \times 10^{-4}$ (bulk) $\text{cm}^{-1}$	—
		$1.1 \times 10^{-3}$ (two surfaces)	—
KCl	Harshaw	$3.3 \times 10^{-4} \text{ cm}^{-1}$	$1.5 \times 10^{-3} \text{ cm}^{-1}$
KCl	Adolf Meller	$3.3 \times 10^{-4} \text{ cm}^{-1}$	$1 \times 10^{-3} \text{ cm}^{-1}$
KCl	Harshaw-Bar	$2.1 \times 10^{-4}$ (bulk) $\text{cm}^{-1}$	$3.7 \times 10^{-4}$ (bulk) $\text{cm}^{-1}$
		$1.0 \times 10^{-4}$ (two surfaces)	$1.2 \times 10^{-4}$ (two surfaces)
KBr	NRL-B212	$1.6 \times 10^{-4}$ (bulk) $\text{cm}^{-1}$	$1.2 \times 10^{-4}$ (bulk) $\text{cm}^{-1}$
		$2.4 \times 10^{-4}$ (two surfaces)	$1.4 \times 10^{-4}$ (two surfaces)
LiF	Harshaw	$2.1 \times 10^{-3} \text{ cm}^{-1}$	$7.4 \times 10^{-4} \text{ cm}^{-1}$
KRS-5	Harshaw	$2.3 \times 10^{-3} \text{ cm}^{-1}$	$3.5 \times 10^{-3} \text{ cm}^{-1}$



Table IX. Absorption Coefficients for Yttralox at DF and HF Wavelengths

Sample	Wavelength ( $\mu\text{m}$ )	$\beta_{\text{total}}$ ( $\text{cm}^{-1}$ )
As received	3.8	$1.4 \times 10^{-2}$
	2.7	$1.4 \times 10^{-2}$
After oxygen treatment	3.8	$2.3 \times 10^{-3}$
	2.7	$3.8 \times 10^{-3}$

Table X. Miscellaneous Oxides

Host	Source	Absorption coefficient ( $\text{cm}^{-1}$ )	
		DF	HF
$\text{Al}_2\text{O}_3$	Crystal Systems	$2.4 \times 10^{-2}$	$3.4 \times 10^{-3}$
$\text{Al}_2\text{O}_3$	Union Carbide	$2.5 \times 10^{-2}$	$2.6 \times 10^{-3}$
$\text{Al}_2\text{O}_3$	AMMRC	$3.4 \times 10^{-2}$	$4 \times 10^{-3}$
MgO	Norton	$5.4 \times 10^{-3}$	$4.0 \times 10^{-2}$
SrTiO <sub>3</sub>	NL Industries	$2 \times 10^{-2}$	$6 \times 10^{-3}$

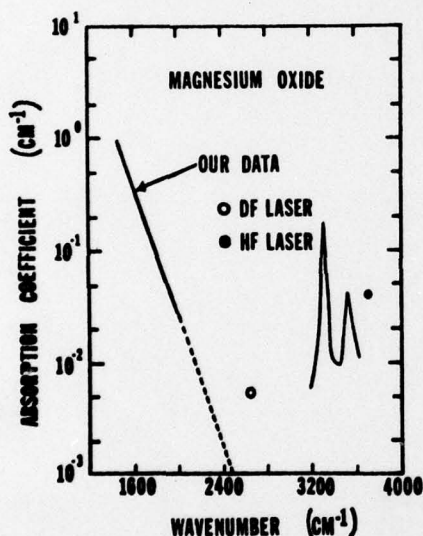


Fig. 3. Intrinsic absorption (straight line) and extrinsic absorption in single crystal MgO (Norton Co.). Extrinsic absorption bands are seen to lie between the DF and HF calorimetric data points.

window for short wavelength lasers. This oxide material is produced by General Electric Corporate Research and Development Laboratories. The data in Table IX indicate the rather high values of  $\beta$  for an initial sample of this material. The reason for this high extrinsic absorption is the presence of strong impurity bands lying directly between the 3.8- $\mu\text{m}$  and 2.7- $\mu\text{m}$  laser lines.<sup>11</sup> These impurity bands, which are presumably associated with oxygen or  $\text{OH}^-$  impurities, are also common to other oxides, e.g., MgO. The reduction of these bands, which clearly limits the absorption coefficients at DF and HF wavelengths, could lower the absorption to near the intrinsic value of  $1 \times 10^{-4} \text{ cm}^{-1}$  at 3.8  $\mu\text{m}$ .

In order to reduce these impurity bands, which might be associated with oxygen vacancies in the material, a

heat treatment of the sample in a small amount of oxygen was attempted in order to drive oxygen into these vacancies making the ceramic more stoichiometric. The initial sample ( $\beta \sim 1.4 \times 10^{-2} \text{ cm}^{-1}$ ) was returned to General Electric for conditioning in a high temperature, oxygen-containing ( $\sim 10 \text{ ppm O}_2$  in argon) atmosphere. On remeasuring the oxygen treated sample, the DF absorption coefficient had been reduced by a factor of 6 and the HF a factor of over 4. From Table IX, however, we see that the material is not yet intrinsic so that further treatments may be necessary to reduce  $\beta$  to its theoretical limit.

#### H. Miscellaneous Oxides

Table X lists results of  $\beta$  for some other common oxides. Sapphire is essentially intrinsic at 3.8  $\mu\text{m}$ , and thus no significant improvement in  $\beta$  is expected. MgO is extrinsically limited by  $\text{OH}^-$  bands lying between the DF and HF region. These bands, which are very similar to those lying between the DF and HF region in Yttralox, are shown in Fig. 3. These data were obtained from a Beckman IR-12 spectrometer. A reduction of these bands should greatly improve the absorption in this material.

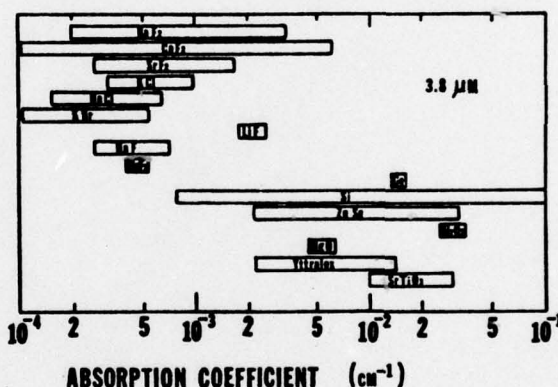


Fig. 4. Range of absorption coefficients in various chemical laser window materials at 3.8  $\mu\text{m}$ .

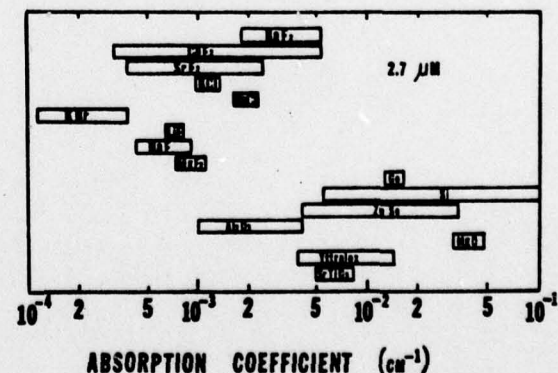


Fig. 5. Range of absorption coefficients in various chemical laser window materials at 2.7  $\mu\text{m}$ .

#### IV. Summary and Conclusions

In the preceding sections, detailed discussions on many of the most likely candidates for use as chemical laser window materials were presented. It is now possible to collect all these data into two composite graphs which represent at the present time the extent of our DF-HF absorption coefficient measurements. Such a composite will enable the reader to determine quickly the range of  $\beta$ 's observed for any particular host studied.

The composite data at DF frequencies are shown in Fig. 4. The bars indicate the range of total (bulk plus surface) absorption measured. Figure 5 shows results for the same samples at HF frequencies.

It is possible to draw cautiously some conclusions about the best potential laser window materials from Figs. 4 and 5. Care is necessary because the absorption is only one of several critical parameters which dictate the effectiveness of the material as a chemical laser window. Therefore, from essentially only an absorption coefficient point of view, one can say that the alkaline earth fluoride and the alkali halides are the best window candidates at this time. The most promising oxide material would be Yttralox, while the semiconducting material of greatest appeal would be ZnSe. These recommendations, as mentioned above, would have to be weighted in terms of other physical parameters en-

tering, for example, the figure of merit for the material<sup>6</sup> in order to obtain the best window. In addition of course, the specific requirements of the application would further limit the choice.

The authors are extremely grateful to the many contributors mentioned in the main text for providing state-of-the-art materials to us for these measurements. This research was supported by the Advanced Research Projects Agency of the Department of Defense and by the ONR Metallurgy Division.

#### References

1. T. F. Deutch, *J. Electron. Mater.* **4**, 663 (1975).
2. M. Hass, J. W. Davisson, H. B. Rosenstock, and J. Babiskin, *Appl. Opt.* **14**, 1128 (1975).
3. M. Hass, J. W. Davisson, P. H. Klein, and L. L. Boyer, *J. Appl. Phys.* **45**, 3959 (1974).
4. J. J. Hinchey and C. M. Banas, *Appl. Phys. Lett.* **17**, 386 (1970).
5. M. Hass, J. W. Davisson, H. B. Rosenstock, J. A. Slinkman, and J. Babiskin, in *Optical Properties of Highly Transparent Solids*, S. S. Mitra and B. Bendow, Eds. (Plenum, New York, 1975).
6. M. Sparks and H. C. Chow, *J. Appl. Phys.* **45**, 1510 (1974).
7. M. L. Meistrich, *J. Phys. Chem. Solids* **29**, 1119 (1968).
8. J. W. Davisson, *J. Mater. Sci.* **9**, 1701 (1974).
9. T. F. Deutch, *J. Phys. Chem. Solids* **34**, 2091 (1973).
10. C. Greskovich and K. N. Woods, *Am. Ceram. Soc. Bull.* **52**, 473 (1973).
11. To be published.

#### OSA TOPICAL MEETING ON OPTICAL OBJECTIVE

This meeting is devoted to optical phenomena, properties, and processes in infrared optical materials. Special emphasis will be given to materials for components (such as windows, lenses, filters, wave guides, modulators, absorbers, and AR and protective coatings) for modern infrared applications (especially in the 3-5- and 10- $\mu$  regimes) such as high-energy laser systems, communications, imaging and scanning, solar energy conversion, infrared detection, and spectroscopy.

#### TECHNICAL SESSIONS

Invited and contributed papers will be presented in such areas as:

- Residual absorption in infrared window materials and coatings
- Temperature, stress, and electric and magnetic field dependence of optical constants of IR materials
- Optical properties of thin films, surfaces, and interfaces
- Scattering of IR radiation from optical surfaces
- Optical phenomena in infrared glasses and amorphous coatings
- Irreversible (catastrophic) laser damage phenomena
- Propagation effects in IR materials, including self focusing and thermally induced lensing and birefringence
- Nonlinear optical processes in IR materials
- Optical properties of pyroelectrics and other IR detector materials
- Influence of impurities and imperfections on optical properties of infrared materials
- Measurement techniques for IR optical properties, especially for low-absorption coefficients, thin film optical constants, infrared scattering, stress optical coefficients and nonlinear susceptibilities
- Solar energy absorbers, stability of selective surfaces at elevated temperatures and high photon fluxes

#### PHENOMENA IN INFRARED MATERIALS CALL FOR CONTRIBUTED PAPERS

Each author should submit both a 25-word abstract for use in the preliminary program and a summary or extended abstract, which will be used as a basis for selection of papers and for making up the conference digest. The summary should contain a minimum of 300 words and a maximum of 500 words of text, figures and tables may be included in addition, but an overall limit of four pages must be adhered to. Since the extended abstract will be photographed directly for the digest, it should be typed clearly on good quality bond paper and conform exactly to the following specifications: use 8 1/2 x 11 inch paper, with one inch margins, type the title in caps and names of author(s) and institute(s) and address(es) in lower case, both centered on the page, followed by the text of the summary, number the pages lightly in pencil. Material from photoduplication machines is not acceptable. The 25-word abstract should begin with the title of the paper followed by name(s) of author(s), address(es), and the text of the abstract. The abstract should be typed on a separate sheet of paper.

All abstracts and summaries must reach us before September 3, 1976.

#### Mail them to:

Optical Society of America  
Optical Phenomena in Infrared Materials  
Suite 620

2000 L Street, N.W.  
Washington, D. C. 20036

Authors will be informed by September 30 of the disposition of their papers.

#### ARRANGEMENTS

The meeting will be held in Annapolis, Maryland, at the Annapolis Hilton. Limousine service is available from the Baltimore-Washington International Airport (formerly Friendship Airport). A bloc of sleeping rooms has been reserved for meeting attendees. Rates are: singles \$24-\$36, doubles \$32-\$44. Annapolis is the capital of Maryland. Many colonial buildings have been restored and are within walking distance of the hotel. Hotel reservation cards and information, along with a copy of the advance

1-3 DECEMBER 1976 ANNAPOLIS, MARYLAND  
program for the meeting, will be sent to all who return the inquiry card. This material will be sent by November 1. The registration fee for the meeting will be \$50.

#### TECHNICAL PROGRAM COMMITTEE

B. Bendow, *Co-chairperson*  
Deputy for Electronic Technology,  
RAJCE/ETSS

Hanscom AFB, MA 01731

S. S. Mitra, *Co-chairperson*  
Department of Electrical Engineering  
University of Rhode Island  
Kingston, RI 02881

F. Abeles  
Laboratoire d'Optique  
Université Paris VI  
Quai St. Bernard  
Paris 5, France

A. S. Barker  
Bell Laboratories  
Whippany Road  
Whippany, NJ 07981

H. E. Bennett  
Naval Weapons Center, C-6018  
China Lake, CA 93555

I. L. Birman  
Physics Department  
City University of New York  
138 & Convent  
New York, NY 10031

B. Lax  
National Magnet Laboratory  
170 Albany Street  
Cambridge, MA 02139

W. C. Spitzer  
Physics Department  
University of Southern California  
Los Angeles, CA 90007

J. Tauc  
Division of Engineering  
Brown University  
Providence, RI 02912



# Infrared bulk and surface absorption by nearly transparent crystals

Herbert B. Rosenstock, Don A. Gregory, and James A. Harrington

We present an analysis of laser calorimetric data that deduces both the bulk and the surface absorption in a single run. The method involves use of long rod geometry combined with an analytical solution of the heat equation for the temperature distribution in a sample that is heated both internally and on the surfaces. Bulk and surface absorption coefficients, heat transfer coefficient, and thermal diffusivity appear as parameters; the last is treated as known, and the thermal rise curve is fitted to the three others. The solution obtained is valid at all points and times, and measurement of the temperature during and after laser heating at different points therefore narrows the possible fit considerably. Examples illustrating the method are presented for ZnSe,  $\text{CaF}_2$ ,  $\text{NaF:Li}$ ,  $\text{NaCl}$ ,  $\text{KBr}$ , and  $\text{KCl}$  at 2.7  $\mu\text{m}$ , 3.8  $\mu\text{m}$ , and 10.6  $\mu\text{m}$ . Surface absorption is found to be dominant in all cases.

## I. Introduction

We have measured the absorption of several almost transparent crystals at several infrared frequencies (see Table I). On account of the weakness of the absorption, the usual direct spectroscopic method, which involves comparison of the intensities of the incoming and outgoing beams, fails, and laser-calorimetry techniques must be used: what is measured at a certain point on the crystal is the temperature rise as a function of time while, and after, the sample is penetrated by a laser beam; this can then be related to the absorption coefficients of the material. That relationship is not wholly straightforward, but sufficiently careful analysis enables us to determine separately both the bulk absorption coefficient and the total absorption at the surfaces. In all cases, we have found the latter to dominate—a consequence, undoubtedly, of the considerable care that has been taken in purifying and perfecting the crystals, thus probably reducing the bulk absorption close to its intrinsic or multiphonon minimum. As the practical motivation for this work is the discovery and preparation of highly transmitting solids (for applications such as windows to a high power laser), the fact that surface rather than bulk absorption is now dominant even for fairly thick crystals is important in guiding further efforts.

In Sec. II we describe our method of analyzing data, show its relation to the more usual simpler techniques, and explain why we believe that the extra effort is worthwhile and indeed essential. In Sec. III we describe our experimental arrangements and our results, and in Sec. IV we discuss their significance. The Appendix contains the dry mathematical detail needed for Sec. II.

## II. Analysis: Temperature Distribution

We need the solution to the following problem in heat conduction: A solid, originally at a uniform temperature, is heated by a source constant in time from time  $t = 0$  to time  $t = t_1$ . What is the temperature at all points and times? This is a classical boundary value problem whose solution is outlined in at least one standard textbook.<sup>1</sup> But, in spite of a recent resurgence of interest,<sup>2-4</sup> we have found no detailed solution of this precise problem suitable for our purposes, and we therefore present it here.

First, however, let us consider the usual simple procedure for inferring absorption coefficients from laser calorimetry data (i.e., temperature vs time curves). There, one assumes small samples and neglects heat losses to the environment; more precisely, it is assumed that absorption of energy anywhere in the sample results instantaneously in a temperature rise that is uniform throughout the sample. The slope of the resulting thermal rise curve alone (rather than the detailed shape of the curve) is then analyzed to yield an average absorption coefficient. This simple procedure ignores all space dependence of the temperature and thus implicitly assumes immediate thermalization. (The heat absorbed is supposedly dispersed uniformly through the sample and in a time shorter than of experimental resolution.) Much obtainable information is in effect

H. B. Rosenstock is with the U.S. Naval Research Laboratory, Washington D.C. 20375; the other authors are with University of Alabama, Huntsville, Alabama 35807.

Received 1 March 1976.



discarded when experimental conditions make that assumption valid. For example, by actually measuring temperature differences as a function of position (rather than assuming that none exist), we can learn about the source of the heat (e.g., bulk vs surface absorption), particularly in samples that are long or thin. The simple analysis is also invalid at very short times (before thermalization can occur) or very long ones (after heat transfer across the boundary is important). Our detailed analysis, which explicitly gives the temperature as a function of both position and time, is therefore particularly useful for irregular geometries (e.g., samples that are long or thin) and for experiments in which time resolution is good.

Accordingly, we solve explicitly the heat equation

$$\nabla^2 T + g/k = (1/\alpha)\partial T/\partial t \quad (1)$$

subject to the boundary conditions

$$k\partial T/\partial n + hT = 0 \quad (\text{all boundaries}) \quad (2)$$

and the initial condition

$$T = 0 \quad (t = 0) \quad (3)$$

at all points in the solid. Here  $t$  means time,  $x, y, z$  are the space coordinates,  $T = T(x, y, z, t)$  is the temperature,  $k$  the thermal conductivity,  $\alpha = k/c\rho$  is called thermal diffusivity,  $c$  and  $\rho$  are the specific heat and density of the solid,  $h$  is the heat transfer coefficient (the rate at which heat is lost across the surface),  $n$  is the space normal at any point on the surface, and  $g(x, y, z, t)$  the source of heat (in our case the heat absorbed from the laser beam traversing the solid). Our general boundary conditions (called boundary conditions of the third kind) reduce to simpler ones when  $h/k$  approach either 0 (second kind—insulated surfaces) or infinity (first kind—a heat bath). Explicit solutions of this system can be obtained for certain coordinate systems (we have done so in rectangular and cylindrical ones) and for certain forms of the source function  $g$ ; the forms of  $g$  for which this is possible are fairly restrictive but correspond closely to what we need in practice. The first restriction we put on  $g$  is on its time dependence: the source must be either on or off and not vary with time in any more complicated way:

$$g(x, y, z, t) = \begin{cases} g_0(x, y, z) & 0 < t < t_1, \\ 0 & \text{otherwise.} \end{cases} \quad (4)$$

$g_0$  can contain both surface and bulk terms, but to allow proceeding further in closed form, the beam profile, i.e., the  $y, z$  dependence of  $g_0$ , must be somewhat restricted. We have found three such profiles. They are a delta function (i.e., an infinitely sharp beam), a step function (i.e., a beam of uniform intensity near the center and 0 elsewhere), and a narrow Gaussian (narrow in the sense that its halfwidth must be appreciably smaller than the cross section of the absorber). Let us write out only the first of these forms:

$$g_0 = P[B + \frac{1}{2}S]\delta(x) + \frac{1}{2}(x - L_x)\delta(y - \frac{1}{2}L_y)\delta(z - \frac{1}{2}L_z). \quad (5)$$

This describes a sharp beam of power density  $P$  traversing a rectangular parallelepiped along its  $x$  axis; the

solid extends through  $0 < x < L_x$ ,  $0 < y < L_y$ ,  $0 < z < L_z$ . Integration of Eq. (5) over the entire solid verifies that  $\beta$  and  $S$  are, respectively, the bulk absorption coefficient (per centimeter) and total fractional absorption by both surfaces (dimensionless). The results are written out in the Appendix and in more detail in Ref. 5. For a detailed derivation, the reader should consult Chap. 2 of Ref. 1, or a similar text. For present purposes, we can write the temperature simply as

$$T(x, y, z, t) = \beta \sum_{mnp} f_{mnp}^{(1)}(x, y, z, t) + S \sum_{mnp} f_{mnp}^{(2)}(x, y, z, t). \quad (6)$$

The point is that the bulk and surface absorption  $\beta$  and  $S$  appear simply as multiplicative constants; the  $f$ 's are known (though fairly complicated) functions depending on the physical parameters  $\rho, k, c, h$ , and the crystal dimensions as well as the indicated space and time coordinates; the sums over  $m, n, p$  contain an infinite number of terms but converge reasonably rapidly. The result appears in the same form for other beam profiles (only the details of the  $f$ 's are different); and the same is true for cylindrical absorbers. [In that case the space coordinates should be called  $(r, z)$  rather than  $(x, y, z)$ , and there are only two instead of three summations.]

The procedure for making measurements is now as follows: attach a thermocouple to a point  $(x, y, z)$  of the solid; measure  $T$  there from time 0 (laser turnon) to some time beyond  $t_1$  (laser cutoff); attempt to fit the resulting curve to Eq. (6) by varying the bulk and surface absorption constants  $\beta$  and  $S$ , thus determining the latter when a fit is obtained. The procedure should then be repeated for placement of the thermocouple at some other point  $(x, y, z)$ ; a different curve will be obtained, but it should be fittable by the same  $\beta$  and  $S$ . We should also mention one unpleasant complication: one parameter entering into the  $f$ 's in Eq. (6), viz., the heat transfer coefficient  $h$ , is not usually known and so must be treated as an unknown, together with  $\beta$  and  $S$ , in the fitting process.

### III. Experimental Techniques and Procedures

Standard laser calorimetric methods<sup>6</sup> were employed to measure the small absorption coefficients at chemical laser frequencies. The experimental setup, which has been described elsewhere in greater detail,<sup>7</sup> consists of an air calorimeter and a small cw DF-HF chemical laser of our own construction.<sup>8</sup> The calorimeter is conventional, see Fig. 1, except for a series of small holes along the bottom that admit a purge gas (dry nitrogen, helium, etc.). In practice, the absorption of HF radiation by air in the calorimeter and subsequent distortion of the heating-cooling curves due to heating of the air have not been detected even without the purge. Purge gas is frequently used, however, to minimize any errors in the temperature-time data and to better characterize the heat transfer coefficient which is of importance in the theoretical prediction of the temperature-time curves.

The samples studied have been procured from a wide variety of window material processors. The contributors in this case were the Naval Research Laboratory,

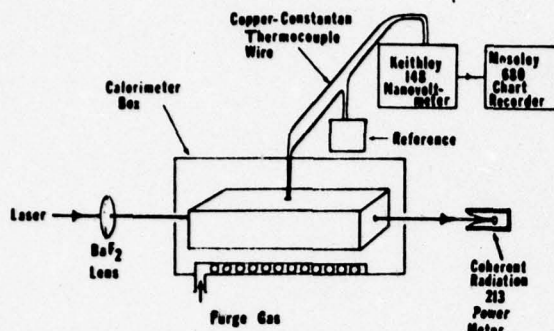


Fig. 1. Schematic experimental arrangement.

Harshaw Chemical Company, and Raytheon Corporation. In most cases, the samples are received with a good surface finish. When this is the case, the samples are run as received. After an initial measurement, the surfaces are examined using Normarski microscopy and then refinished. Mechanical polishing involves a final polish with Linde B and isopropanol with intermediate polishes using diamond grit for the harder substances. For ZnSe the prescriptions of Hughes Research Lab<sup>9</sup> and Raytheon<sup>10</sup> for chemical etching on pitch laps were utilized.

Surface cleaning just prior to measurement is one of the most important requirements for a reliable absorption coefficient. Crystals washed with CH-bonded solvents like methanol, ethanol, acetone, etc., which have absorptions<sup>11</sup> in the DF-HF region, show higher absorption coefficients than crystals washed in, for example, carbon tetrachloride. At present, all samples have a final cleaning with spectrograde CCl<sub>4</sub> just prior to measurement.

Measurements were made on several crystals and three frequencies. A sample of the data is shown in Fig. 2. Here the solid curves are the experimental measurements on a ZnSe sample about 6 × 1 × 1 cm in size; the points are the best fit obtainable by varying the parameters  $h/k$ ,  $\beta$ , and  $S$ . All other parameters are treated as known.<sup>12,13</sup> The upper curve is a run taken with the thermocouple at the center of the surface ( $x = 3$  cm), the lower one with the thermocouple near the end ( $x = 1$  cm). In the course of the analysis,  $h/k$  is first determined by fitting to the curve beyond the laser cutoff (because at those times, no further absorption is taking place and the changes in temperature are therefore largely due to the surface heat losses and no longer strongly dependent of the other unknowns,  $\beta$  and  $S$ ). Then the early parts of the curves are fitted by varying the bulk and surface absorption coefficients. Once this is optimized, further improvements are usually possible by changing  $h$  again and repeating the process. The reader will note that very good fits are possible to either curve, but not to both simultaneously with the same parameters. This, of course, points to the importance of making temperature measurements at more than one point if convincing values of the absorption coefficients are to be obtained. Results are summarized in Table I.

Table I. Bulk Absorption Coefficient and Total Surface Absorption of Several Crystals at Three Wavelengths

	Bulk absorption coefficient (cm <sup>-1</sup> ) 10 <sup>3</sup> $\beta$	Surface absorption (dimensionless) 10 <sup>4</sup> $S$	Heat transfer coefficient (cm <sup>-1</sup> ) 10 <sup>3</sup> $h/k$
2.7 $\mu$ m			
KBr	5	190	1
ZnSe	50-140	60-900	2
CaF <sub>2</sub>	20	350	20
NaF:LiF	80	350	4
3.8 $\mu$ m			
ZnSe	110	280	1-2
CaF <sub>2</sub>	25	270	32
NaCl	90	4000	60
10.6 $\mu$ m			
KBr	12	420	1
KCl	8	90	2

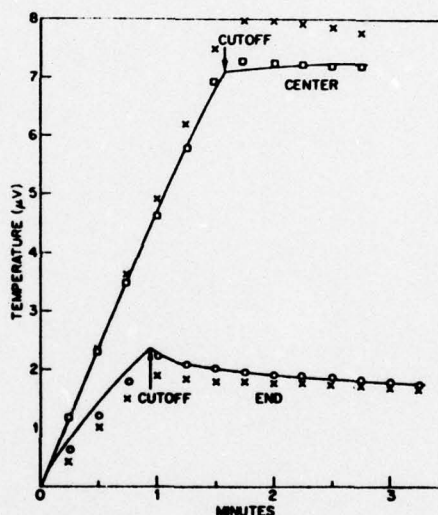


Fig. 2. Sample of data (ZnSe at 2.7  $\mu$ m). Solid curves are experimental results: the upper for measurement at the center of the lateral surface; the bottom for measurement on a point on the lateral surface near an end surface. Individual points indicate attempted analytical fits by Eq. (6). While excellent fits are obtainable for each curve separately (squares and circles, respectively), the best to both curves (crosses) show 10% deviations. See Table II.

Table II.

	Bulk absorption coefficient 10 <sup>3</sup> $\beta$ (cm <sup>-1</sup> )	Surface absorption 10 <sup>4</sup> $S$ (dimensionless)	Heat transfer coefficient/ thermal conductivity 10 <sup>3</sup> $h/k$ (cm <sup>-1</sup> )
□	146	0	0.6
○	135	380	4.0
×	135	200	2.0



#### IV. Discussion

In discussing our data as summarized in Table I, let us first consider the last column which gives the heat transfer coefficient (divided by the presumably known thermal conductivity). This is not a quantity of primary interest to us, but must be determined because it is not available in the literature. It has two components, a radiative and a convective one, of which the latter is believed to be the more important. It is also the latter that is most uncertain and probably responsible for the wide variations in the third column. It would appear that convection currents arise inside the calorimeter, unpredictably, at some times and not at others. Furthermore, the great changes in the effective heat transfer coefficients from one run to the next also suggest the likelihood of variations during one run, in contradiction to the implied assumption in our derivation that the heat transfer is constant in any one run. Two conclusions must therefore be drawn from the large variations shown in the last column of Table I: first, that the results in the other two columns, which are of greater physical interest, are not wholly reliable either on account of the unpredictable variations in the heat transfer coefficient (although we should in fairness point out that the data are much less sensitive to changes in the heat transfer coefficient than they are to changes in the absorption coefficients), and, second, the importance of working in the future with an evacuated calorimeter in which the convective and variable heat transfer coefficient will be reduced to nearly zero, and only the radiative part which indeed should remain constant will be left. In one case, KBr at 2.7  $\mu\text{m}$ , we were able to reduce the heat transfer coefficient to a point at which it was no longer troublesome by filling the calorimeter with He rather than air.

The first two columns of numbers, the bulk and surface absorption coefficients, also show considerable variation and should therefore be considered tentative. It is not easy to quote limits on the errors in these quantities with confidence. The dependence of the calculated results on the heat transfer coefficient is complicated (as explained in the Appendix) although fortunately not strong; that on the absorption coefficients is simpler, viz., multiplicative, as seen from Eq. (6). Thus, a 10% deviation from the experimental curves, as in Fig. 2, should translate directly into a 10% uncertainty in  $\beta$ ,  $S$ , or both. Yet things are not that simple: often, an excellent fit can be obtained from one set of parameters for one time interval (e.g., for the first 30 sec after laser cuton), but a different set of  $\beta$ ,  $S$ ,  $h$  is needed for a fit at other times (e.g., after cutoff). Furthermore, in the absence of measurements at different points, the possibility that even a good fit for all times may be fortuitous cannot be excluded. Accordingly, we would be reluctant to claim precision better than within 20%.

Nonetheless, certain physically realistic conclusions can be drawn. The major one is the dominance, at all three frequencies, of surface effects. In every case, the total surface absorption is considerably larger than the bulk absorption of several centimeters of crystal. One

point that does not appear clearly from Table I, but must be made plain here, is the dependence of our results not only on the substance used, but on the particular crystal; variations, not shown in Table I, were obtained for crystals of nominally the same composition, but different preparation and surface treatment. The fact that in each case the surface absorption is equivalent to many cm of bulk absorption indicates that the over-all success of growing pure crystals in bulk has been considerable, and that improving the surface quality of crystals is now the most important task before us toward the goal of producing substances whose over-all absorption will be minimal.<sup>14</sup>

We thank P. H. Klein (NRL) for providing us with most of the samples measured, M. Hass (NRL) for many discussions, and J. M. Rowe (University of Alabama) for his data at 10.6  $\mu\text{m}$ .

This work was sponsored by the Defense Advanced Research Projects Agency and the Office of Naval Research.

#### Appendix: Particular Solution to the Heat Equation

In Sec. II, the appropriate heat flow problem was formulated and the solution given schematically. Here we summarize the details.

The solution is

$$T(x,y,z,t) = (P/k) \sum_{m,n,p} (Z_m^2 Z_n^2 Z_p^2 / \gamma_{mnp}) \cdot u(\epsilon_m, x) u(\epsilon_n, y) u(\epsilon_p, z) \cdot (P_1 \beta + P_2 S) u(\epsilon_n, L_y/2) u(\epsilon_p, L_z/2) \cdot \psi_{mnp}(t).$$

Here  $P$  is the power density of the laser beam,  $H = h/k$ ,

$$\psi_{mnp}(t) = \begin{cases} 1 - \exp(-\alpha \gamma_{mnp} t) & 0 < t < t_1 \\ \exp(-\alpha \gamma_{mnp} t) [\exp(+\alpha \gamma_{mnp} t_1) - 1] & t > t_1 \end{cases}$$

$$P_1 = (H/\epsilon_m)(1 - \cos L_x \epsilon_m) + \sin L_x \epsilon_m,$$

$$P_2 = \epsilon_m(1 + \cos L_x \epsilon_m) + H \sin L_x \epsilon_m,$$

$$\gamma_{mnp} = \epsilon_m^2 + \epsilon_n^2 + \epsilon_p^2,$$

and  $L_x$  is the length of the sample.

The  $\epsilon_m$  are the positive solutions of

$$\tan \epsilon_m L_x = 2H\epsilon_m / (\epsilon_m^2 - H^2),$$

and the  $u(\epsilon_m, x)$  and  $Z_m$  are given by

$$u(\epsilon_m, x) = \epsilon_m \cos \epsilon_m x + H \sin \epsilon_m x$$

$$Z_m^2 = 2/[2H + L_x(\epsilon_m^2 + H^2)].$$

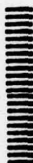
To obtain the  $\epsilon$ ,  $u$ , and  $Z$  with subscripts  $n$  (or  $p$ ) instead of  $m$ , replace  $x$  by  $y$  (or  $z$ ) in the above expressions.

The position  $(x,y,z)$  enters the expression for the temperature  $T(x,y,z,t)$  through the functions  $u$ ; time  $t$ , through  $\psi(t)$ ; and the parameters describing the sample size  $(L_x, L_y, L_z)$ , conductivity  $k$ , heat transfer coefficient  $h$  through the eigenvalues. The reader should consult Ref. 5 for solutions applicable to other situations [to sources other than the  $g_0$  of Eq. (5) and to cylindrical geometries] and Ref. 1 for a more general theory of the heat equation.



## References

1. N. Ozisik, *Boundary Value Problems of Heat Conduction* (International Textbook Co., Scranton, Pa., 1968).
2. E. Bernal G., Appl. Opt. 14, 314 (1975).
3. K. T. White and L. E. Midwinter, Optoelectronics 5, 323 (1973).
4. A. Kahane and L. H. Skolnik, in *Proceedings Fifth Conference on Laser Window Materials, November 1975*, C. R. Andrews and C. L. Strecker, Eds. (University of Dayton Research Institute Press, Dayton, Ohio, 1976).
5. H. B. Rosenstock, in "High Energy Laser Windows," Semiannual Report 6 on ARPA Order 2031 (Naval Research Laboratory, Washington, D.C., 30 September 1975), p. 15.
6. M. Haas, J. W. Davisson, P. H. Klein, and L. L. Boyer, J. Appl. Phys. 45, 3959 (1974).
7. M. Haas, J. W. Davisson, H. B. Rosenstock, and J. Babiskin, Appl. Opt. 14, 5 (1975).
8. J. A. Harrington, Final Technical Report, contract DAAH01-74-C-0438, prepared for U.S. Army Missile Command, Redstone Arsenal, Alabama (March 1975).
9. M. Braunstein, in *Third Conference on High Power Infrared Laser Window Materials, February 1974*, C. A. Pitha and B. Bendow, Eds. (University of Dayton Research Institute Press, Dayton, Ohio, 1975), p. 863.
10. C. B. Willingham, Semi-Annual Technical Report, ARPA order 2415 (March 1974).
11. *Sadtler Standard Spectra* (Sadtler Research Laboratories, Philadelphia, 1968).
12. Y. S. Toloukian and E. H. Buyco, Eds., *Thermophysical Properties of Matter: Vol. 5, Specific Heat; TPRC Data Series, Thermophysical Research Corporation* (Plenum, New York, 1970).
13. *Optical Materials, Raytran ZnSe*, private publication of Raytheon Research Division, Waltham, Mass.
14. J. W. Davisson, J. Mater. Sci. 9, 1071 (1974).



## Meetings Schedule OPTICAL SOCIETY OF AMERICA 2000 L Street N.W., Washington D.C. 20036

17-18 September 1976 OPTICAL FABRICATION AND TESTING ROAD SHOW, Rochester, New York Information: J. W. Quinn at OSA or CIRCLE NO. 55 ON READER SERVICE CARD

18-23 October 1976 ANNUAL MEETING, Convention Center, Tucson, Arizona (Braniff Place Hotel) Information: J. W. Quinn at OSA or CIRCLE NO. 61 ON READER SERVICE CARD

5-6 November 1976 OPTICAL FABRICATION AND TESTING ROAD SHOW, Auburn, Massachusetts Information: J. W. Quinn at OSA or CIRCLE NO. 63 ON READER SERVICE CARD

1-3 December 1976 OPTICAL PHENOMENA IN INFRARED MATERIALS, OSA TOPICAL MEETING, Annapolis, Maryland Information: J. W. Quinn at OSA or CIRCLE NO. 57 ON READER SERVICE CARD

13-15 December 1976 ATMOSPHERIC AEROSOLS, THEIR OPTICAL PROPERTIES AND EFFECTS, OSA TOPICAL MEETING, Williamsburg, Virginia Information: J. W. Quinn at OSA or CIRCLE NO. 58 ON READER SERVICE CARD

22-24 February 1977 OPTICAL FIBER TRANSMISSION 2, OSA TOPICAL MEETING, Williamsburg, Virginia Information: J. W. Quinn at OSA or CIRCLE NO. 56 ON READER SERVICE CARD

9-14 October 1977 ANNUAL MEETING, Royal York, Toronto, Canada Information: J. W. Quinn at OSA or CIRCLE NO. 64 ON READER SERVICE CARD

30 October-3 November 1978 ANNUAL MEETING, Jack Tar Hotel, San Francisco Information: J. W. Quinn at OSA or CIRCLE NO. 53 ON READER SERVICE CARD

7-12 October 1979 ANNUAL MEETING, Holiday Inn/Flagship, Rochester, New York Information: J. W. Quinn at OSA or CIRCLE NO. 54 ON READER SERVICE CARD

# Infrared absorption limits of HF and DF laser windows\*

M. Hass

Naval Research Laboratory, Washington, D.C. 20375

J. A. Harrington and D. A. Gregory

University of Alabama in Huntsville, Huntsville, Alabama 35807

J. W. Davisson

Naval Research Laboratory, Washington, D.C. 20375

(Received 13 February 1976)

The infrared absorption coefficients of NaCl, KCl, NaF, CaF<sub>2</sub>, and BaF<sub>2</sub> have been determined by calorimetric techniques at the laser wavelengths 1.06, 2.7, and 3.8  $\mu\text{m}$ . The absorption level of the best crystals can be  $10^{-5} \text{ cm}^{-1}$  or lower at 1.06  $\mu\text{m}$ , but no crystal with a coefficient lower than  $10^{-4} \text{ cm}^{-1}$  at 2.7 and 3.8  $\mu\text{m}$  has been found. Possible reasons for these results are discussed.

PACS numbers: 78.50.Ec, 42.70.Fh, 42.80.Em, 78.20.Dj

Windows for infrared lasers can undergo optical distortion or fracture at high cw power levels due to their finite absorption coefficient.<sup>1,2</sup> The absorption coefficients of various candidate laser window crystals are reported here at the HF chemical laser wavelength of 2.7  $\mu\text{m}$ , the DF chemical laser wavelength of 3.8  $\mu\text{m}$ , and at the Nd:YAG laser wavelength of 1.06  $\mu\text{m}$ . An examination of this and other data suggests the presence of excess absorption at the HF and DF laser wavelengths relative to that at both higher and lower wavelengths.

The determination of the absorption coefficients of highly transmitting materials can be a difficult experimental problem due to the low magnitude of absorption coefficient and possible interference from surface effects and scattering. The most widely used method involves the measurement of the temperature as a function of time of a sample which is irradiated by an intense laser source (often referred to as the thermal rise or laser calorimetric method).<sup>3</sup> By use of axial irradiation with a long-rod geometry, it becomes possible to separate out surface and bulk absorption.<sup>4</sup> The first measurements employing this approach for studying a number of pure samples over a wide wavelength range are reported here.

The origin of the residual infrared absorption in highly transmitting crystals can be associated with several different mechanisms. On the high-frequency side of the reststrahlen band, intrinsic multiphonon absorption associated with mechanical or electric anharmonicity can occur.<sup>5,6</sup> This has been observed to have a charac-

teristic decreasing exponential dependence as a function of frequency in a large number of crystals.<sup>7</sup> Departures from this exponential dependence are generally associated with impurities, surface effects, and difficulties of measurement. The present investigation focuses on this region where the intrinsic absorption is below the limit of observation at the present time.

In the measurements reported here at 1.06  $\mu\text{m}$ , absorption coefficients in the  $10^{-5} \text{ cm}^{-1}$  region, and occasionally lower, have been obtained in some crystals. In addition, inspection of the thermal rise curves indicates that little or no surface absorption is present. Since interference effects from scattering might be expected to be strongest at the shortest wavelength, it is believed that these 1.06- $\mu\text{m}$  measurements provide an indication of the lower limit of the coefficient in a particular sample.

The experimental results for a number of samples are summarized in Table I along with data at 5.3  $\mu\text{m}$  on similar samples reported elsewhere.<sup>8</sup> Many other samples of these and other crystals showing higher absorption coefficients were also studied, but will be presented elsewhere.<sup>9</sup> The data for crystals of KCl and BaF<sub>2</sub>, which have the lowest loss at 5.3  $\mu\text{m}$ , are shown in Fig. 1. It can be seen both from Table I and Fig. 1 that the absorption at both 1.06 and 5.3  $\mu\text{m}$  can be at the  $10^{-5} \text{ cm}^{-1}$  level. On the other hand, no crystal with a coefficient lower than  $10^{-4} \text{ cm}^{-1}$  at 2.7 and 3.8  $\mu\text{m}$  has ever been observed. Here a number of good crystals of KCl and KBr were studied. They are among the lowest

TABLE I. Absorption coefficients of crystals at various laser wavelengths.

Crystal	Source	Absorption coefficient ( $\text{cm}^{-1}$ )			
		1.06 $\mu\text{m}$ <sup>a</sup>	2.7 $\mu\text{m}$ <sup>b</sup>	3.8 $\mu\text{m}$ <sup>b</sup>	5.3 $\mu\text{m}$ <sup>c</sup>
KCl	NRL	$7 \times 10^{-6}$	$3.7 \times 10^{-4}$	$2.1 \times 10^{-4}$	
KCl					$1.5 \times 10^{-5}$
KBr	NRL B-305	$< 3 \times 10^{-6}$	$1.2 \times 10^{-4}$	$2.2 \times 10^{-4}$	
CaF <sub>2</sub>	Hughes (polycrystal forging)	$4 \times 10^{-5}$	$1.8 \times 10^{-4}$	$2.7 \times 10^{-4}$	
BaF <sub>2</sub>	Harshaw	$3 \times 10^{-5}$	$5.2 \times 10^{-4}$	$4.4 \times 10^{-4}$	$< 3 \times 10^{-5}$

<sup>a</sup> Measured at NRL on rods using a Nd:YAG laser.

<sup>b</sup> Measured at University of Alabama-Huntsville on rods using

a multiline gas laser.

<sup>c</sup> Measured at Raytheon and reported in Ref. 8.



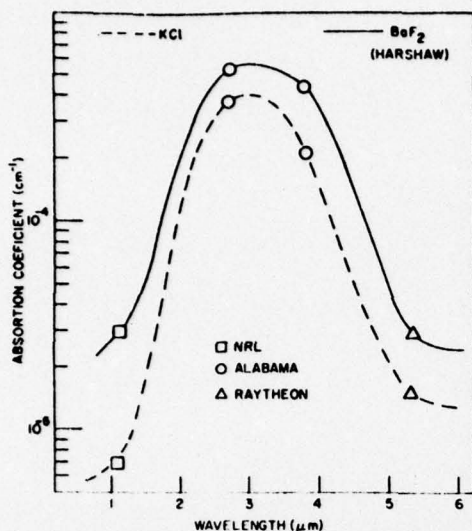


FIG. 1. Bulk absorption coefficient of KCl and BaF<sub>2</sub> as a function of wavelength.

ever reported at the CO<sub>2</sub> laser wavelength of 10.6  $\mu\text{m}$ . While the crystals studied at 5.3  $\mu\text{m}$  were not the same as those employed in this investigation, the measurements reported at that wavelength are sufficiently low so that the trend shown in Fig. 1 can be established with some degree of confidence and could hold for the other good crystals as well.

Thus, the data imply excess absorption at 2.7 and 3.8  $\mu\text{m}$  in the better crystals compared to the absorption at both higher and lower wavelengths. Furthermore, this appears to hold so far for a number of alkali halide and alkaline earth fluoride crystals which are the most transparent of the candidate laser window materials. The origin of this absorption has not yet been established, but a number of possibilities such as the following can be suggested.

In the infrared region of the spectrum, molecular impurity complexes are the most common source of excess bulk absorption away from the region where intrinsic effects predominate. In particular, the stretching mode of the OH ion gives rise to a characteristic absorption band near 2.7  $\mu\text{m}$  in alkali halide crystals.<sup>10</sup>

While the OH concentration as evidenced by the ultra-violet absorption at 0.2  $\mu\text{m}$  is small<sup>11</sup> or undetectable in the best crystals, contributions from this origin cannot be completely excluded. Similarly, the 3.8- $\mu\text{m}$  region, the wings of the 3.5- $\mu\text{m}$  band associated with the stretching modes of CH impurities, might be responsible. While such impurities can be readily observed on the surface of crystals arising from polishing vehicles (and can be removed by proper cleaning procedures),<sup>8</sup> it is possible that there may be bulk contributions as well. This would be possible to check if a sensitive broad-band technique such as spectral emittance were available. While the sensitivity of such techniques is adequate, interference from surfaces and scattering still presents problems at low absorption levels.

In conclusion, the results presented here suggest that absorption in the best presently available window materials at the important chemical laser wavelengths of 2.7 and 3.8  $\mu\text{m}$  is limited to  $10^{-4} \text{ cm}^{-1}$ , and this may be associated with OH and CH impurities. If the impurity bands were eliminated, absorption levels in the  $10^{-5} \text{ cm}^{-1}$  region should be attainable with crystals of present optical quality.

The authors are grateful to P.H. Klein for supplying some of the crystals used in this investigation.

\*Research sponsored in part by the ONR Material Sciences Division.

<sup>1</sup>M. Sparks, J. Appl. Phys. **42**, 5029 (1971); M. Sparks and H.C. Chow, J. Appl. Phys. **45**, 1510 (1974).

<sup>2</sup>J.R. Jasperse and P.D. Gianino, J. Appl. Phys. **43**, 1686 (1972); B. Bendow and P.D. Gianino, J. Electron. Mater. **2**, 87 (1973).

<sup>3</sup>L.H. Skolnick, in *Optical Properties of Highly Transparent Solids* (Plenum, New York, 1975), p. 405.

<sup>4</sup>M. Hass, J.W. Davissson, H.B. Rosenstock, and J. Bablskin, Appl. Opt. **14**, 1128 (1975).

<sup>5</sup>T.C. McGill, in *Optical Properties of Highly Transparent Solids* (Plenum, New York, 1975), p. 3.

<sup>6</sup>L.L. Boyer, J.A. Harrington, M. Hass, and H.B. Rosenstock, Phys. Rev. B **11**, 1665 (1975).

<sup>7</sup>T.F. Deutsch, J. Phys. Chem. Solids **34**, 2091 (1973).

<sup>8</sup>T.F. Deutsch, J. Electron. Mater. **4**, 663 (1975).

<sup>9</sup>J.A. Harrington, D.A. Gregory, and W. Ott, Appl. Opt. (to be published).

<sup>10</sup>M.L. Meistrich, J. Phys. Chem. Solids **29**, 1111 (1968);

B. Fritz, F. Lüty, and J. Anger, Z. Phys. **174**, 240 (1963).

<sup>11</sup>P.H. Klein (unpublished).



# Extrinsic absorption in KCl and KBr at CO<sub>2</sub> laser frequencies\*

J. M. Rowe and J. A. Harrington

The University of Alabama in Huntsville, Huntsville, Alabama 35807

(Received 2 February 1976; in final form 19 July 1976)

Extrinsic absorption has been studied in KCl and KBr using the technique of tunable CO<sub>2</sub> laser calorimetry. The transparency of these hosts is limited by an extrinsic absorption mechanism common to both KCl and KBr. In particular, an extrinsic absorption band near 9.6  $\mu\text{m}$  in both materials has been studied in detail. The features of this band are compared to a recent theory on impurity induced absorption at CO<sub>2</sub> wavelengths. A bulk absorption in KBr of  $1 \times 10^{-5} \text{ cm}^{-1}$  at 10.6  $\mu\text{m}$  was measured for the best sample—the lowest value observed to date for any material at this frequency.

PACS numbers: 78.50.Ec, 63.20.-c, 78.30.Gt

The alkali halides have been widely studied for their potential as windows on high-powered CO<sub>2</sub> lasers. The transparency, however, of two very promising materials, KCl and KBr, is limited by extrinsic (surface, impurity, mechanical defect, etc.) absorption at the CO<sub>2</sub> frequencies. For KCl, which has been more thoroughly studied at these wavelengths, the measured total absorption coefficient  $\beta$  is two or three times greater than the intrinsic (multiphonon) absorption of  $8 \times 10^{-5} \text{ cm}^{-1}$  at 10.6  $\mu\text{m}$  while at shorter wavelengths the discrepancy between measured and intrinsic absorption is even greater.<sup>2</sup> The situation for KBr is even more extreme due to the very small intrinsic absorption ( $2 \times 10^{-7} \text{ cm}^{-1}$  at 10.6  $\mu\text{m}$ ) at CO<sub>2</sub> wavelengths.<sup>1</sup> In order to improve our understanding of the extrinsic absorption mechanisms, the absorption has been measured in KCl and

KBr using the technique of tunable CO<sub>2</sub> laser calorimetry. These measurements have enabled us to (i) obtain more information on an extrinsic absorption band that is observed in KCl near 9.6  $\mu\text{m}$ ,<sup>1,3</sup> (ii) make the first observation (calorimetrically) of a comparable extrinsic band in KBr, and (iii) compare this extrinsic peak in both hosts to recent theoretical work on impurity-induced absorption in alkali halides at CO<sub>2</sub> wavelengths. In addition, for KBr, tunable calorimetry performed on long bar-shaped samples has resulted in the extraction of bulk absorption coefficients near  $1 \times 10^{-5} \text{ cm}^{-1}$ —the lowest value of  $\beta$  obtained to date at 10.6  $\mu\text{m}$  in any material.

The samples were grown using the reactive atmosphere process (RAP)<sup>2</sup> and represent some of the highest-purity crystals available. To minimize surface absorption, chemical etching techniques<sup>4</sup> were applied to KCl and a light polish on a chamois with isopropanol was used for KBr. Conventional laser calorimetric methods were used to measure the small absorption coefficients.<sup>2</sup>  $\beta$  was obtained as a function of frequency using a CO<sub>2</sub> laser tunable from 9.55 to 10.76  $\mu$  with single line powers from 1 to 9 W.

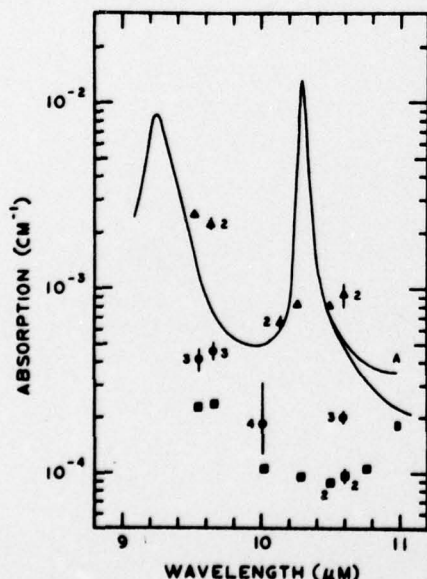


FIG. 1. Total absorption in KBr and KCl at 300 K. Experimental points for an older KCl sample ( $\Delta$ ) and recent RAP-grown KCl ( $\circ$ ) and KBr ( $\square$ ) are shown. The solid curve is the absorption calculated by Duthler (Ref. 3) for KCl (curve A) and KBr (curve B) with 0.03 ppm each of  $\text{SO}_4^{2-}:\text{Mg}^{+2}$ ,  $\text{NO}_3^-$ , and  $\text{HCO}_3^-$ . Numbered points indicate the results of more than one measurement.

Figure 1 shows the total absorption coefficient in KCl and KBr as a function of wavelength at 300 K. Experimental points for two samples of KCl and one of KBr are compared with a recent theoretical calculation due to Duthler,<sup>5</sup> which is shown as a solid line. The experimental data were taken on several different samples of KCl. The higher absorbing sample ( $\Delta$ ) was grown several years ago by early RAP techniques and reflects the greater strength of the impurity band present in these materials near 9.6  $\mu\text{m}$ . More recent RAP-grown KCl ( $\circ$ ) and KBr ( $\square$ ) produced by P. Klein of the Naval Research Laboratory clearly shows the decrease in the 9.6- $\mu\text{m}$  absorption band as well as a decrease in the over-all absorption at 10.6  $\mu\text{m}$ . The theory curve represents total absorption for the host material plus 0.03 ppm each of  $\text{SO}_4^{2-}:\text{Mg}^{+2}$ ,  $\text{NO}_3^-$ , and  $\text{HCO}_3^-$ . At 9.3 and 10.3  $\mu\text{m}$ , the  $\text{SO}_4^{2-}:\text{Mg}^{+2}$  and  $\text{HCO}_3^-$  ions, respectively, produce sharp absorption peaks in the extrinsically limited wings of the multiphonon tail. From a comparison of the theory and experimental data, it is evident that the 10.3  $\mu\text{m}$  absorbing impurities considered by

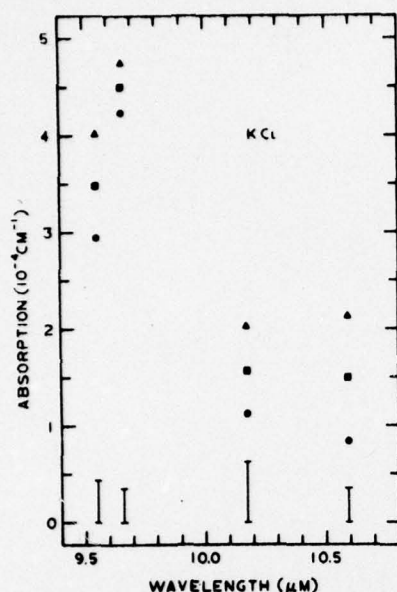


FIG. 2. Total absorption in KCl as a function of wavelength at 100 K (●), 200 K (■), and 300 K (▲). Error bars at the bottom of the figure represent one standard deviation, and apply to all measurements at a given wavelength.

Duthler are insufficient by themselves to account for the observed extrinsic band near 9.6  $\mu\text{m}$ .

Others have discussed the impurity absorption in this region for KCl,<sup>2,3,6</sup> but the corresponding band in KBr has not been observed before by tunable laser calorimetry in high-quality samples. Stierwalt and Hass<sup>6</sup> suggest this extrinsic absorption is a surface effect while Lipson *et al.* indicate that  $\text{ClO}_3^-$ , an ion not considered by Duthler, absorbs strongly in the 10.6- $\mu\text{m}$  region. An independent analysis of the impurity content of the sample was not practical and, thus, correlation between specific impurities present in our samples and the 9.6  $\mu\text{m}$  absorption in KCl or KBr was impossible. We can conclude, however, that the extrinsic band most likely arises from the same source in both KCl and KBr since the band appears near 9.6  $\mu\text{m}$  in each host but the source is not one or a combination of the ions considered by Duthler in this theory. Possibly the inclusion of additional impurities such as  $\text{ClO}_3^-$  in the theory would produce absorption peaks nearer the observed band.

The behavior of the absorption near 9.6  $\mu\text{m}$  has also been measured in KCl as a function of temperature, using a liquid-nitrogen cryostat constructed for this purpose. The results are shown in Fig. 2. The data indicate that the peak absorption is essentially independent of temperature. This agrees with the observations made by Deutsch<sup>5</sup> from 300 to 80 K.

The extrinsic absorption may take place in the bulk of the sample or on the surface. Additional information about the extrinsic absorption in KBr was obtained by separating the bulk absorption component from total absorption. This was accomplished using the method due to Hass *et al.*,<sup>7</sup> in which a long bar-shaped sample

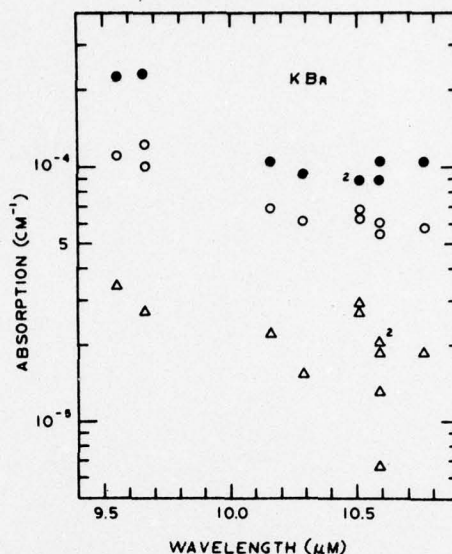


FIG. 3. Absorption for two samples of KBr at 300 K and several wavelengths. Both the total (●) and bulk-only (○) absorption are shown for one sample. The bulk only absorption for a better sample (Δ) is also shown. Numbered points indicate the result of more than one measurement.

is used. Measurement of the small temperature rise, which results from passing the laser beam through the length of the sample, is made at the middle of the rod. Heat generated at the end surfaces of the rod, where the beam enters and exits, takes longer to reach the middle than bulk heating from the filament of laser light down the axis of the rod. Therefore, initial heating is an indication of bulk absorption. The results from two different samples of KBr at 300 K and for several wavelengths are shown in Fig. 3. Near 9.6  $\mu\text{m}$ , one sample exhibits increased absorption for the bulk (○) and a larger increase for total absorption (●). A better sample also shows some rise in bulk absorption (Δ) at 9.6  $\mu\text{m}$ , although the data are more scattered. In this sample, the bulk absorption is  $1 \times 10^{-5} \pm 50\%$   $\text{cm}^{-1}$  at 10.6  $\mu\text{m}$ . This represents the lowest absorption measured to date at this wavelength.

An important conclusion can be drawn from this data. In both KBr samples the extrinsic absorption band near 9.6  $\mu\text{m}$  is present in the bulk absorption only. This means that this extrinsic band in KBr is not due entirely to surface absorption, but is in fact due to a source present in the bulk, as well as on the surface of the sample.

The data presented indicate the high degree of transparency in state-of-the-art KCl and KBr window materials. Nevertheless, an extrinsic absorption band appears near 9.6  $\mu\text{m}$  that limits the absorption at 10.6  $\mu\text{m}$ . We have shown that, although no assignment of this absorption to a specific impurity can be made from our data, the extrinsic absorption is present in both surface and bulk absorption and that the common extrinsic band in KCl and KBr is not due to any impurity discussed by Duthler.



\*This research was supported by the Advanced Research Projects Agency of the Department of Defense and by the Office of Naval Research, Metallurgy Division.

<sup>1</sup>T. F. Deutsch, J. Phys. Chem. Solids **34**, 2091 (1973).

<sup>2</sup>M. Hass, J. W. Davisson, P. H. Klein, and L. L. Boyer, J. Appl. Phys. **45**, 3959 (1974).

<sup>3</sup>T. F. Deutsch, Appl. Phys. Lett. **25**, 109 (1974); H. G. Lipson, J. J. Larkin, and B. Bendow, J. Electron. Mater. **4**, 51 (1975); P. J. Shlichta, R. E. Chaney, and J. Yee, in Fourth Annual Conference on Laser Window Materials, Tucson, Arizona, 1974 (unpublished).

<sup>4</sup>J. W. Davisson, J. Mater. Sci. **9**, 1701 (1974).

<sup>5</sup>C. J. Duthler, J. Appl. Phys. **45**, 2668 (1974); C. J. Duthler, in Fourth Annual Conference on Laser Window Materials, Tucson, Arizona, 1974 (unpublished).

<sup>6</sup>D. L. Stierwalt and M. Hass, in Fourth Annual Conference on Laser Window Materials, Tucson, Arizona, 1974 (unpublished).

<sup>7</sup>M. Hass, J. W. Davisson, H. B. Rosenstock, J. A. Slinkman, and J. Babiskin, in *Optical Properties of Highly Transparent Solids*, edited by S. S. Mitra and B. Bendow (Plenum, New York, 1975), p. 435; M. Hass, J. W. Davisson, H. B. Rosenstock, and J. Babiskin, Appl. Opt. **14**, 1128 (1975).

# INFRARED ABSORPTION IN $\text{ThO}_2$ -DOPED $\text{Y}_2\text{O}_3$

James A. Harrington\*  
University of Alabama in Huntsville  
Huntsville, Alabama 35807

and

C. Greskovich  
Corporate Research and Development  
General Electric Company  
Schenectady, New York 12301

The optical absorption has been measured over the 2-4  $\mu\text{m}$  region in dense, polycrystalline  $\text{Y}_2\text{O}_3$  containing 10 mole %  $\text{ThO}_2$  in solid solution. Measurements of the absorption coefficient ( $\beta$ ) in  $\text{ThO}_2$ -doped  $\text{Y}_2\text{O}_3$  indicated an intrinsic (multiphonon) level of  $2.6 \times 10^{-5} \text{ cm}^{-1}$  at DF(3.8  $\mu\text{m}$ ) wavelengths although calorimetrically obtained  $\beta$ 's were in the low  $10^{-3} \text{ cm}^{-1}$  region for the best materials. This difference is attributed to extrinsic absorption mechanisms and, in particular, to an impurity band of as yet undetermined origin lying directly between the DF and HF frequencies. Various ceramic processing techniques were applied to sintered  $\text{ThO}_2$ -doped  $\text{Y}_2\text{O}_3$  ceramic to reduce this absorption with the most successful being a high temperature anneal in a higher partial pressure of oxygen.



## INFRARED ABSORPTION IN $\text{ThO}_2$ -DOPED $\text{Y}_2\text{O}_3$

### I. INTRODUCTION

During the past several years there has been increasing interest in the optical properties of highly transparent materials at infrared laser wavelengths. This interest in low loss materials has been stimulated in part by the need for solid windows and other transparent optical components on high-powered infrared lasers. At the DF (3.8  $\mu\text{m}$ ) and HF (2.7  $\mu\text{m}$ ) chemical laser wavelengths a wide range of materials present themselves for consideration as potential laser windows.<sup>1</sup> In particular, oxides show great promise owing to their favorable mechanical properties although their optical absorption is generally not as low as that for the alkali halides and alkaline earth fluorides.<sup>1</sup> In an effort to explore the potential of new materials for laser windows, a study has been made of the infrared absorption in  $\text{ThO}_2$ -doped,  $\text{Y}_2\text{O}_3$ .<sup>2</sup>

Sintered  $\text{Y}_2\text{O}_3$  containing 10 mole %  $\text{ThO}_2$  in solid solution<sup>3</sup> is a cubic, polycrystalline ceramic characterized by relatively high strength, resistance to environmental attack, and good infrared transparency. In investigations to date, however, these properties have not been exploited for applications as infrared laser windows; instead most interest has centered on the laser action in

$\text{Nd}^{3+}$ -doped material.<sup>4,5</sup> One reason for this is that the residual absorption in oxide materials transparent at DF and HF wavelengths is often an order of magnitude or more greater than the residual absorption in alkali halides or alkaline earth fluorides at the same wavelengths.<sup>1</sup> Initially, therefore, these materials were neglected in favor of the simpler and better characterized halide and fluoride crystals and only more recently have oxides received much attention.

The higher absorption of oxides in the transparent regime results from two different sources. Intrinsic absorption arising from multiphonon processes ultimately limits the absorption in any perfect crystal. For the oxides this level of absorption can be appreciable in the 2 to 4  $\mu\text{m}$  region because of the high energies of the vibrational modes in these compounds. For example,  $\text{Al}_2\text{O}_3$  has an intrinsic absorption of  $1 \times 10^{-2} \text{ cm}^{-1}$  at 3.8  $\mu\text{m}^1$  and thus sapphire has exhibited only limited usefulness as a DF laser window.  $\text{MgO}$  and  $\text{ThO}_2$ -doped  $\text{Y}_2\text{O}_3$ , however, have considerably lower intrinsic absorption levels and thus show greater promise as low loss materials. The other source of absorption is that due to extrinsic absorption mechanisms. These can be chemical impurities, mechanical imperfections, or surfaces - all of which can make a substantial contribution to the total absorption. In the oxides, a particularly troublesome source is the



$\text{OH}^-$  impurity which gives rise to extrinsic absorption bands near  $2.7 \mu\text{m}$ . These bands, which have been observed in  $\text{ThO}_2$ -doped  $\text{Y}_2\text{O}_3$  and  $\text{MgO}$ ,<sup>1</sup> increase the total absorption well above the intrinsic value and thus an understanding of the source of this contaminant and techniques to eliminate it from the host are important for improved optical quality.

In order to reduce the level of the extrinsic absorption in  $\text{ThO}_2$ -doped  $\text{Y}_2\text{O}_3$ , several different physical treatments of the material were utilized. These were, in turn, correlated at various stages with the optical absorption which thus enabled us to determine the effect of processing and retreatment of the sintered material on the infrared absorption coefficient. In this manner a retreatment process was developed which reduced the absorption in untreated material by as much as a factor of 6 at DF wavelengths. Even with this reduction, however, the total absorption, which has been reduced to about  $2 \times 10^{-3} \text{ cm}^{-1}$  at  $3.8 \mu\text{m}$ , is still above the intrinsic value.

## II. EXPERIMENTAL PROCEDURES

### A. Material's preparation

A composition of  $\text{Y}_2\text{O}_3 + 10\% \text{ ThO}_2$  was prepared by an oxalate precipitation approach described elsewhere.<sup>3</sup> After calcination at  $800^\circ\text{C}$ , the resulting oxide powder was sometimes ball-milled to reduce aggregate and particle

size and improve chemical homogeneity. At other times this step was omitted from the overall ceramic processing. The ball-milled powders yielded sintered specimens that were optically water clear, whereas samples prepared from unmilled, calcined powder exhibited veiling. Samples produced from both unmilled and ball-milled powder were studied optically in an effort to correlate any differences observed in the absorption with this step in the processing. The remaining ceramic powder processing, forming, and heat treatment procedures are those described in connection with the fabrication of  $\text{ThO}_2$ -doped  $\text{Y}_2\text{O}_3$  ceramics containing neodymium for lasing behavior.<sup>3</sup> All samples were sintered in dry  $\text{H}_2$  (dew point  $\approx -70^\circ\text{C}$ ) at  $2170^\circ\text{C}$  followed by cooling in the presence of wet  $\text{H}_2$  (dew point  $\approx 25^\circ\text{C}$ ). If equilibration of the sintered samples with the oxygen in wet  $\text{H}_2$  ceases at  $\sim 1600^\circ\text{C}$ , then it is estimated that the effective oxygen partial pressure "seen" by the samples is about  $10^{-11}$  atm.

#### B. Optical absorption measurements

The samples measured ranged in size from approximately  $1 \times 0.5 \times 0.3$  cm to large discs 5 cm in diameter by 0.5 cm thick. The surfaces were polished using diamond grit and just prior to measurement the samples were carefully cleaned in spectrograde  $\text{CCl}_4$  to reduce surface absorption. Scattering in heavily veiled samples presented some problem although this could be reduced somewhat by careful align-



ment of the optical beam through the center of the crystal where veiling was often less prevalent.

The infrared absorption at room temperature was measured using a Beckman IR-12 spectrophotometer. The spectra recorded were useful in determining the characteristic multiphonon edge of  $\text{ThO}_2$ -doped  $\text{Y}_2\text{O}_3$  as well as for obtaining information about the extrinsic absorption whenever the strength of this absorption was greater than approximately  $10^{-2} \text{ cm}^{-1}$ . In general, conventional infrared spectroscopy was useful for measuring absorption coefficient  $\beta$  down to the  $10^{-2} \text{ cm}^{-1}$  range but below this other methods had to be employed to measure the very low absorptions common to high quality, low loss laser window materials.

In order to measure the small absorption at DF and HF chemical laser frequencies, standard laser calorimetric methods were employed.<sup>6</sup> The experimental arrangement consisted of a vacuum or air calorimeter and a small cw DF-HF chemical laser constructed by one of us (JAH). The laser delivers 5 to 10 watts of multiline cw HF and DF power which is quite adequate for obtaining reliable temperature-time data.

A three-slope method<sup>6</sup> is applied to the data for the calculation of  $\beta$ . The absorption coefficient calculated in this conventional manner is the total absorption coefficient representing the sum of the bulk and surface contributions. Although it is possible to abstract only the

bulk contribution,<sup>7,8</sup> this was found unnecessary in this study. The reason for this is that the fractional power absorbed at the surfaces is generally about  $10^{-4}$ /surface which is much smaller than the  $10^{-3} \text{ cm}^{-1}$  total absorption coefficients measured for the best  $\text{ThO}_2$ -doped  $\text{Y}_2\text{O}_3$ . The surface contribution in  $\text{ThO}_2$ -doped  $\text{Y}_2\text{O}_3$  is therefore negligible, and thus the measured total  $\beta$  is adequate for the discussions of extrinsic and intrinsic absorption mechanisms.

### III. RESULTS AND DISCUSSION

The infrared absorption of thin plates of  $\text{ThO}_2$ -doped  $\text{Y}_2\text{O}_3$  was measured routinely by Greskovich and Woods<sup>3</sup> and then later studied in greater detail by Harrington, et al.<sup>1</sup> Since these studies, additional samples have been measured to provide further information about the nature of the extrinsic absorption in this material. Figure 1 gives the absorption coefficient  $\beta$  as a function of wavenumber at room temperature for a 2" diameter by 0.5 cm thick disk of  $\text{Y}_2\text{O}_3$  containing 10 mole %  $\text{ThO}_2$  in solid solution. This particular sample had unusually good optical quality as it was prepared from ball-milled powder. From this data, the intrinsic absorption can be estimated at the chemical laser wavelengths. Deutsch<sup>9</sup> has shown experimentally and others have confirmed theoretically,<sup>10</sup> that  $\log \beta$  is proportional to energy for energies two to six times



greater than the reststrahl energy. The straight solid line in Fig. 1 is the experimental data confirming this dependence for  $\text{ThO}_2$ -doped  $\text{Y}_2\text{O}_3$  ceramic just as has been done by Deutsch<sup>9</sup> for many other solids. The dashed extension of this line is an extrapolation which can be extended to the DF ( $\sim 2630 \text{ cm}^{-1}$ ) and HF ( $\sim 3570 \text{ cm}^{-1}$ ) wavelengths in order to obtain the intrinsic (multiphonon) absorption coefficient. The extrapolated multiphonon edge yields,

$$\begin{aligned}\beta_{\text{int}} (\text{DF}) &= 2.6 \times 10^{-5} \text{ cm}^{-1} \\ \beta_{\text{int}} (\text{HF}) &= 4.6 \times 10^{-9} \text{ cm}^{-1}.\end{aligned}$$

These absorption coefficients thus represent the approximate limiting value for  $\text{ThO}_2$ -doped  $\text{Y}_2\text{O}_3$  at chemical laser wavelengths. Additional  $\log \beta$  versus energy curves made for different  $\text{ThO}_2$ -doped  $\text{Y}_2\text{O}_3$  samples prepared from both unmilled and ball-milled powder have yielded similar results for the extrapolated intrinsic values.

The calorimetrically measured absorption coefficients at DF and HF wavelengths, however, are several orders of magnitude greater than these intrinsic values. As explained in the Introduction this is due to extrinsic absorption present in the samples. In  $\text{ThO}_2$ -doped  $\text{Y}_2\text{O}_3$  solid solution, one source of this extrinsic absorption is clearly shown in Fig. 1 as a band lying between the DF and HF laser frequencies. This absorption band is the major contri-

bution to the total absorption measured at chemical laser frequencies since this absorption "tails" into the DF and HF region with a strength much greater than  $\beta_{\text{int}}$ .

The most probable source of the extrinsic band is hydrogen or oxygen related defects.  $\text{OH}^-$  defects have been studied in many solids<sup>11</sup> and it is found that the infrared stretching mode occurs near the HF laser frequency. Oxides are particularly prone to  $\text{OH}^-$  contamination and similar extrinsic bands have been observed in  $\text{MgO}$ .<sup>1</sup> Since the last step in the ceramic processing involves sintering in dry hydrogen followed by cooling in wet  $\text{H}_2$ , it is not unlikely that the final  $\text{ThO}_2$ -doped  $\text{Y}_2\text{O}_3$  solid solution could contain some dissolved hydrogen. If hydrogen were in the form of  $\text{H}^-$  ions, high lying vibrational modes approximately two times greater than the highest energy band modes would be expected. By analogy, however, with the fundamental mode of vibration of  $\text{H}^-$  ions in a variety of solids,<sup>12</sup> the  $\text{H}^-$  ion vibration in  $\text{ThO}_2$ -doped  $\text{Y}_2\text{O}_3$  should be well below the  $3300 \text{ cm}^{-1}$  average frequency of the extrinsic band. Therefore,  $\text{H}^-$  ions are an unlikely source of this impurity band. Interstitial  $\text{O}^{2-}$  ions (caused by the substitution of  $2 \text{ Th}^{4+}$  for  $\text{Y}^{3+}$  ions<sup>5</sup>) and possibly a very small fraction of oxygen vacancies (caused by the low partial pressure of oxygen in the sintering atmosphere) are other possible sources of absorption. Also,  $\text{S}^{2-}$  ions can be present in the solid solution because they are



known to be picked-up during ball-milling.<sup>3</sup> While the specific identification of these impurities in ThO<sub>2</sub>-doped Y<sub>2</sub>O<sub>3</sub> with infrared absorption bands has not been made, it is possible to obtain some indirect information which will help to eliminate certain ions as the likely extrinsic source.

In an attempt to study the role of oxygen in the extrinsic absorption, a ball-milled sample of 10% Th<sub>2</sub>-doped Y<sub>2</sub>O<sub>3</sub> was retreated (oxidized) at high temperature (~2000°C) in an argon atmosphere having a partial pressure of oxygen ~10<sup>-5</sup> atm (10 ppm). Before the sample was retreated, an extrinsic band like that shown in Fig. 1 was evident and the DF and HF absorption coefficients were as given in Table 1. After the retreatment described above, the extrinsic band had completely disappeared as measured on the infrared spectrometer and the DF and HF absorptions were lowered by factors of 6 and 4, respectively. Table 1 summarizes the  $\beta$  measurements. During refiring in a higher partial pressure of oxygen, oxygen presumably diffuses into the cubic solid solution while possibly hydrogen or other impurity species simultaneously diffuse out of the sample. In addition, the number of oxygen vacancies should decrease by consideration of the pertinent equations for point defect equilibria. By annealing the sample in a higher partial pressure of oxygen, the extrinsic absorption is reduced appreciably but the reduced  $\beta$ 's are

still extrinsically limited as can be seen by comparing them with  $\beta_{int}$ . This particular sample was then annealed again in a higher oxygen partial pressure  $\sim 2 \times 10^{-1}$  atm (air) in an attempt to reduce the absorption even further. Unfortunately, the sample reacted with the alumina support at  $1740^{\circ}\text{C}$ , abruptly ending this series of experiments.

While it would seem that the most likely contaminants would be removed in the above annealing procedure, sulfur species might be more resistant to removal. Sulfur contamination can occur in the ball-milling operation because the ball-mill is rubber lined. Greskovich and Woods<sup>3</sup> have determined the amount of sulfur in ball-milled and unmilled starting powder and suggested that even after sintering some sulfur may remain in the polycrystalline solid. In an effort to determine if this impurity may lead to the increased optical absorption a series of samples identical in every respect except that half were prepared from ball-milled powder and half from unmilled powder were measured. The samples prepared from unmilled powder were veiled whereas the other samples from ball-milled powder were optically clear.

The infrared spectra for all four samples listed in Table 2 exhibited infrared spectra essentially identical to that shown in Fig. 1 and thus they are not reproduced here. In particular, each sample had an easily observable extrinsic absorption band of approximately the strength



shown in the figure except for the small, unmilled sample which was so veiled that scattering dominated the absorption spectra obscuring the impurity band. The calorimetrically determined absorption coefficients are given in Table 2. A comparison of the  $\beta$ 's for the two 2 inch samples and for the two small samples, which did not have the good optical quality of the larger samples, indicate that the absorption is smallest in the samples prepared from ball-milled powder. This is not what would be expected if sulfur ions were the source of absorption. Therefore, we cannot conclude that sulfur introduced by the ball-milling operation leads to higher absorption coefficients.

#### IV. CONCLUSIONS

The optical properties of a solid solution of  $Y_2O_3 + 10$  mole %  $ThO_2$  have been studied in relation to ceramic processing techniques. Although the intrinsic absorption coefficient at DF wavelengths was found to be very low ( $2.6 \times 10^{-5} \text{ cm}^{-1}$ ), the absorption coefficients measured calorimetrically were more than 100 times greater. The source of the higher absorption was connected with an extrinsic absorption band appearing between the DF and HF frequencies. Characterization of this absorption band involved correlating the absorption with certain ceramic

processing procedures. High temperature annealing in a higher partial pressure of oxygen proved most successful in reducing this absorption band. During this retreatment oxygen apparently diffused into the ceramic solid solution and probably reduced the oxygen vacancy concentration and the impurity concentration of foreign ions such as  $\text{OH}^-$ .

#### ACKNOWLEDGMENTS

The authors are grateful to D. A. Gregory, C. Patty, and L. Kan for assistance in the optical measurements. This research has been supported in part by ONR Metallurgy Division, the Advanced Research Projects Agency of the Department of Defense and the General Electric Company.

\* After January 1, 1977, permanent address, Hughes Research Laboratory, Malibu, CA 90265

## REFERENCES

1. J. A. Harrington, D. A. Gregory, and W. F. Otto, Appl. Opt. 15, 1953 (1976).
2. Previously Yttralox, a registered product of the General Electric Co.
3. C. Greskovich and K. N. Woods, Bull. Am. Ceram. Soc. 52, 473 (1973).
4. C. Greskovich and J. P. Chernoch, J. Appl. Phys. 44, 4599 (1973).
5. ibid, 45, 4995 (1974).
6. M. Hass, J. W. Davisson, P. H. Klein, and L. L. Boyer, ibid 45, 3959 (1974).
7. M. Hass, J. W. Davisson, H. B. Rosenstock, J. A. Slinkman, and J. Babiskin, in Optical Properties of Highly Transparent Solids, S. S. Mitra and B. Bendow, Eds. (Plenum, New York, 1975).
8. H. B. Rosenstock, D. A. Gregory, and J. A. Harrington, Appl. Opt. 15, 2075 (1976).
9. T. F. Deutsch, J. Electron. Mater. 4, 663 (1975).
10. See for example, L. L. Boyer, J. A. Harrington, M. Hass, and H. B. Rosenstock, Phys. Rev. B 11, 1665 (1975) and references cited therein.
11. B. Wedding and M. V. Klein, Phys. Rev. 177, 1274 (1969).
12. A. S. Barker and A. J. Sievers, Rev. Mod. Phys. 47, Suppl. No. 2 (1975).



TABLE I. Absorption coefficients for sintered  $\text{ThO}_2$ -doped  $\text{Y}_2\text{O}_3$  (prepared from ball-milled powder before and after retreatment in an atmosphere of higher oxygen activity).

Sample Condition	DF ( $3.8\mu\text{m}$ )	FH ( $2.7\mu\text{m}$ )
1. As prepared, fired in $\text{P}_{\text{O}_2} \approx 10^{-11}$ atm; extrinsic absorption seen in IR spectra	$0.014 \text{ cm}^{-1}$	$0.014 \text{ cm}^{-1}$
2. Annealed in $\text{P}_{\text{O}_2} \approx 10^{-5}$ atm; no extrinsic absorption seen in IR spectra	$0.0023 \text{ cm}^{-1}$	$0.0038 \text{ cm}^{-1}$

TABLE 2. Comparison of optical absorption in sintered  $\text{ThO}_2$ -doped  $\text{Y}_2\text{O}_3$  prepared from ball-milled or unmilled starting powder. Samples fired in  $P_{\text{O}_2} \approx 10^{-5}$  atm.

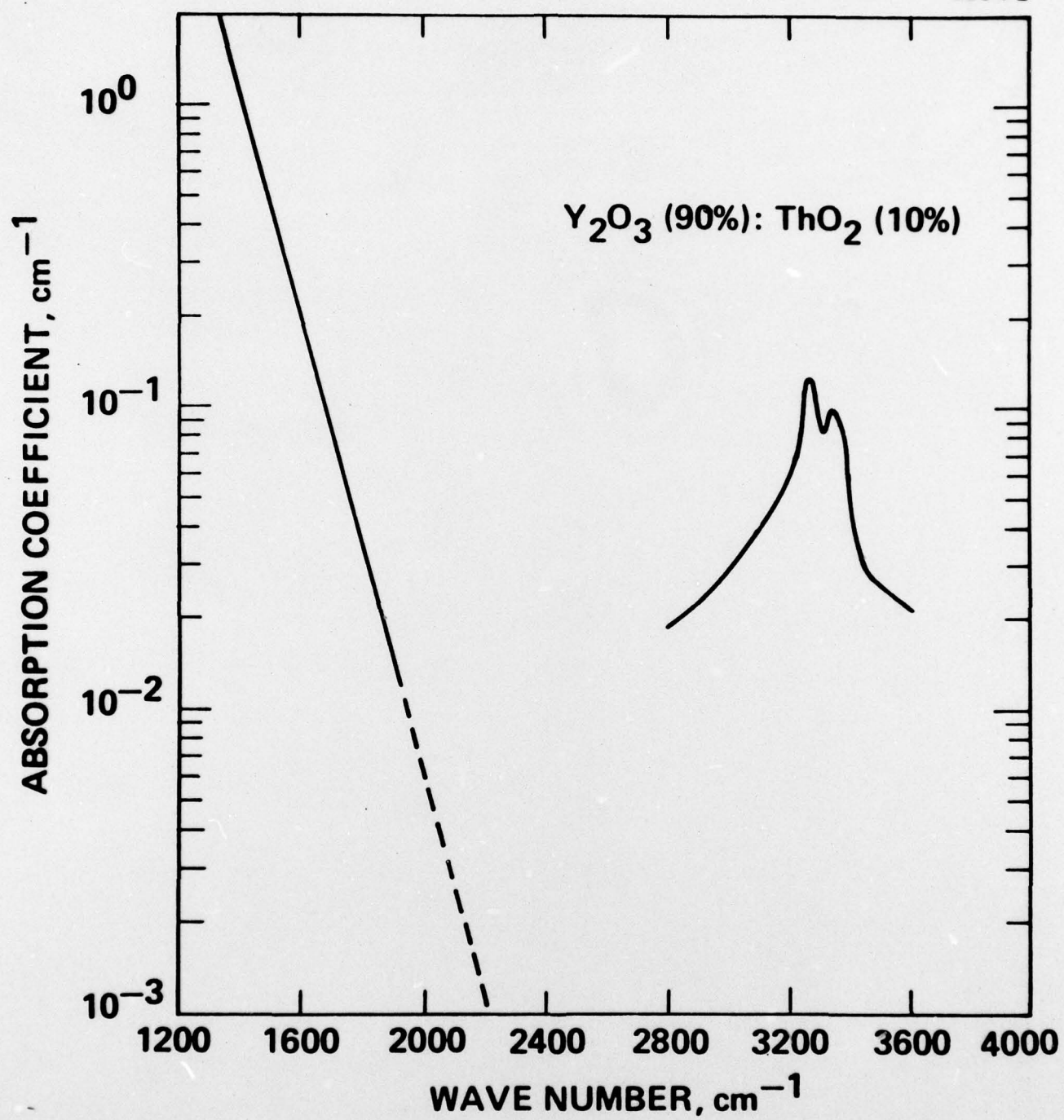
Sample	Starting Powder	DF (3.8 $\mu\text{m}$ )	HF (2.7 $\mu\text{m}$ )
2 in. diam, veiled	unmilled	0.020 $\text{cm}^{-1}$	0.028 $\text{cm}^{-1}$
2 in. diam, clear	ball-milled	0.0022 $\text{cm}^{-1}$	0.0043 $\text{cm}^{-1}$
small, veiled	unmilled	0.037 $\text{cm}^{-1}$	0.067 $\text{cm}^{-1}$
small, clearer	ball-milled	0.017 $\text{cm}^{-1}$	0.049 $\text{cm}^{-1}$

CAPTION

Fig. 1 Absorption coefficient versus wavenumber at room temperature for dense, polycrystalline  $\text{Y}_2\text{O}_3$  containing 10 mole %  $\text{ThO}_2$  in solid solution. Sample fired in  $\text{P}_{\text{O}_2} \approx 10^{-11}$  atm.



5294-2



### CONCLUSION

Throughout this contract period, many materials and experimental methods have been investigated and utilized. It is our opinion that this information should lead to further improvements in the material fabrication area as well as make pertinent information about the absorption of a variety of materials available to the consumer.

Further investigation is needed into several areas including more experimental work in the area of long bar calorimetry. It is our hope that the investigation presented here will lead to other in depth studies in this area.